2017

TUMOR-INTRINSIC INFLAMMATORY PATHWAYS ASSOCIATED WITH TUMOR DORMANCY AND RECURRENCE

Savannah E. Butler

TUMOR-INTRINSIC INFLAMMATORY PATHWAYS ASSOCIATED WITH TUMOR DORMANCY AND RECURRENCE

A thesis submitted in partial fulfillment of the requirements for the degree of Master of Science at Virginia Commonwealth University.

by

SAVANNAH ELIZABETH BUTLER
Bachelor of Science, The College of William and Mary, 2014

Director: MASOUD H. MANJILI, DVM, PHD
PROFESSOR OF MICROBIOLOGY AND IMMUNOLOGY

Virginia Commonwealth University
Richmond, Virginia
May 1, 2017

Acknowledgements

First, I would like to thank my parents for supporting me and encouraging me to follow my passion for science throughout my entire life. Their never-ending support is paramount to my graduate school success and any success I may obtain in the future.

Next, I would like to thank those who worked alongside me in the lab: Timothy Smith and Hussein Aqbi. Their comradery and overall assistance in the lab contributed greatly to my thesis work.

I would also like to acknowledge my committee members: Dr. Michael Idowu and Dr. Kathleen McCoy, who graciously agreed to serve on my graduate advisory committee, despite their busy schedules. Their intellectual contribution enriched my graduate research and graduate education as a whole.

Finally, I would like to thank my advisor, Dr. Masoud Manjili, for his guidance and wisdom throughout my project. His knowledge and expertise was fundamental to my research and I greatly appreciate all the time he spent working with me. I would also like to thank him for encouraging me to pursue my Ph.D., which will allow me to continue my career in biomedical research.

Table of Contents

List of Figures iv

Abbreviations v

Abstract ix

Introduction 1

Materials and Methods 15

Results:

Chloroquine prolongs ADR-induced tumor dormancy in MMC 24

Dormant and relapsing MMC show unique inflammatory signature 26

L-glutamine-addiction increases the rate of relapse in MMC 29

ADR-treated shNF-κB p65 exhibit reduced growth and a reduced rate of relapse *in vitro* and *in vivo* 32

shNF-κB p65 show increased neu expression in response to ADR treatment *in vitro* and *in vivo* 34

shNF-κB p65 show augmented tumor-infiltrate and reduced anti-tumor response 37

CRISPR-Cas9 complete knockdown of NF-κB p65 in MMC 39

Discussion 41

Future Directions 48

References 49

List of Figures

Figure 1: ADR induces tumor dormancy in MMC, *in vitro*.....25

Figure 2: Dormant MMC exhibit unique gene signature compared to relapsing MMC.....27

Figure 3: Inflammatory gene signature during dormancy and relapse 28

Figure 4: Secretion of inflammatory cytokines during dormancy, *in vitro*.....30

Figure 5: L-Glutamine addiction in MMC results in increased rate of relapse.....31

Figure 6: NF-κB p65 knockdown in MMC reduces the rate of relapse, *in vitro*.....33

Figure 7: shNF-κB p65 tumors show reduced growth in response to ADR treatment, *in vivo*.....35

Figure 8: shNF-κB p65 show higher upregulation of neu in response to ADR treatment.....36

Figure 9: shNF-κB p65 tumors display alteration of tumor infiltrate *in vivo* and T cell activation *ex vivo*.....38

Figure 10: CRISPR-Cas9 knockout of NF-κB p65 in MMC 39

List of Abbreviations

ADR: Adriamycin

ANG1: Angiopoietin

AMPKα1: Adenosine monophosphate-activated protein kinase α1

BAFFR: B-cell activation factor

BMP7: Bone morphogenetic protein 7

CQ: Chloroquine

Cas9: CRISPR associated protein 9

CRISPR: Clustered regularly interspaced short palindromic repeats

CRT: Calreticulin

CTC: Circulating tumor cells

CXCL1: CXCL10: C-X-C motif chemokine 1

CXCL2: CXCL10: C-X-C motif chemokine 2

CXCL3: CXCL10: C-X-C motif chemokine 3

CXCL10: C-X-C motif chemokine 10

CXCL12: C-X-C motif chemokine 12

CXCR4: C-X-C chemokine receptor type 4

CXCR7: C-X-C chemokine receptor type 7

DCs: Dendritic cells

DTC: Disseminated tumor cells

EDTA: Ethylenediaminetetraacetic acid

EMT: Epithelial to mesenchymal transition

ER: Estrogen receptor

FACS: Fluorescence-activated cell sorting

FACS buffer: 2mL PBS with 2% FBS, 0.1% sodium azide

FBS: Fetal bovine serum

GFP: Green fluorescent protein

GLN: Glutamine

GLUT1: Glucose transporter 1

GM-CSF: Granulocyte-macrophage colony-stimulating factor

HER-2: Human epidermal growth factor receptor-2

HIF-1: Hypoxia-inducible transcription factor

HMGB1: High mobility group box-1

ICD: Immunogenic cell death

IFN: Interferon

IκB: Inhibitor of NF-kB

IL-1: Interleukin 1

IL-1β: Interleukin 1 beta

IL-2: Interleukin 2

IL-6: Interleukin 6

IL-8: Interleukin 8

IL-12: Interleukin 12

IPA: Ingenuity Pathway Analysis

JNK: 4/c-Jun NH2-terminal kinase

L-glut: L-glutamine

LPS: Lipopolysaccharides

LTβR: Lymphotoxin β-receptor

MAP: Mitogen-activated protein

MAPK: Mitogen-activated protein kinase

MHCI: Major histocompatibility complex 1

MKK4: Mitogen-activated protein kinase 4/c-Jun NH2-terminal-activating kinase

MMC: Mouse mammary carcinoma cell line

MMP: Matrix metalloproteinases

MOI: Multiplicity of infection

NGF: Nerve growth factor

NF-kB: Nuclear factor kappa-light-chain-enhancer of activated B cells

NK: Natural Killer

NSAIDS: Nonsteroidal anti-inflammatory drugs

p38: p38 mitogen-activated protein kinase

p53: Tumor suppressor p53

PBS: Phosphate-buffered saline

PD-L1: Programmed death-ligand 1

PCa: Prostate cancer cell

PGE_2: Prostaglandins E_2

PI: Propidium iodine

Rae-1: Retinoic acid early inducible 1

Raf-Mek-ERK: Mitogen-activated protein kinase (MAPK) cascade

ROS: Reactive oxygen species

PR: Progesterone receptor

RANTES: Chemokine (C-C motif) ligand 5

RPMI: RPMI 1640 with 2mM L-glutamine and 10% fetal bovine serum

SDF-1: Stem cell factor-1

SEM: Standard error of the mean

shRNA: Short hairpin RNA

STAT3: Signal transducer and activator of transcription 3

STAT5: Signal transducer and activator of transcription 5

TAM: Tumor-associated macrophage

TGF-β: Transforming growth factor-β

TLR3: Toll-like receptor 3

TME: Tumor microenvironment

TNF-α: Tumor necrosis factor alpha

TWEAK: Tumor necrosis factor ligand superfamily member 12

uPar: Urokinase receptor

VCAM-1: Vascular cell adhesion protein 1

VEGF-A: Vascular endothelial growth factor A

Abstract

Tumor-intrinsic inflammatory pathways associated with tumor dormancy and recurrence

By Savannah Elizabeth Butler

A thesis submitted in partial fulfillment of the requirements for the degree of Master of Science at Virginia Commonwealth University.

Virginia Commonwealth University, 2017

Director: Masoud H. Manjili, DVM, PhD
Professor of Microbiology and Immunology

The successful treatment of breast cancer is limited due to a fraction of tumor cells escaping drug-treatment by entering a dormant state, only to relapse years or decades later at distant sites. Host-driven chronic inflammatory cells such as M2 macrophages play an important role in tumorigenesis, but the role of tumor-intrinsic inflammatory signaling involved in tumor dormancy and recurrence is unknown. We sought to determine the role of tumor-intrinsic inflammatory pathways in mouse mammary carcinoma cells (MMC) treated with Adriamycin (ADR), a clinically relevant chemotherapeutic drug. We found that ADR-induced dormant tumor cells autonomously produced pro-inflammatory cytokines, *in vitro*. MMC treated with Chloroquine (CQ) prior to ADR treatment displayed a delay in relapse, or prolonging of dormancy, when compared to ADR-treated MMC. Additional gene array data showed predicated activation of NF-κB p65 in ADR-treated dormant MMC that eventually relapsed. These data suggest that the anti-inflammatory function of CQ led to prolonged dormancy. To test this, we investigated the role of inflammatory signaling pathways directly by shRNA-mediated

knockdown and CRISPR-Cas9-mediated knockout of NF-κB p65 in MMC. We found that knockdown of NF-κB p65 resulted in fewer dormant cells after ADR treatment and reduced rate of relapse, *in vitro*. NF-κB p65 was also found to reduce the immunomodulatory effects of ADR, with shNF-κB p65 showing increased upregulation of neu upon ADR treatment. Additionally, we found NF-κB p65 to be associated with a higher infiltration of CD8+ T cells and anti-tumor T cell responses. Our findings suggest a dual role of tumor-intrinsic NF-κB p65 pathway, allowing for escape from drug treatment through dormancy which leads to relapse, but also for proper lymphocyte infiltration and subsequent anti-tumor activity.

Introduction

Breast cancer treatment and recurrence

Despite advancements in cancer treatment and prevention, breast cancer incidence has continued to rise in recent years, with nearly 12.4% of women becoming diagnosed with breast cancer at some point in their lifetime (1). In 2016 alone, it was estimated that 40,450 women died from breast cancer, though the 5-year survival rate reached an all-time high of 89.7%, largely due to the increase in effective treatments. Despite this overall increase in survival, roughly 62% of deaths occur after the 5 year survival mark due to local and distant recurrence (1). Adjuvant therapies, such as chemotherapy and radiation, are thought to prevent local recurrence and metastasis by targeting residual tumor cells following removal of the primary tumor (2). However, such therapies are most effective when the disease is diagnosed early, while only detectable in the primary organ without metastasis, and despite its success, thousands of women continue to relapse years or decades after successful treatment of primary tumors (3).

It is generally recognized that the development of endocrine therapy has proven to be a highly effective method in prolonging survival while also preventing recurrence, though not all breast cancer subtypes are responsive to such therapies (4). Prior to the development of hormone therapies, human epidermal growth factor receptor-2 positive (HER2+) breast cancer was associated with poor prognosis compared to other hormone receptor-positive subtypes, such as estrogen receptor positive (ER+) and progesterone receptor positive (PR+) breast cancers (5). The use of trastuzumab, an anti-HER2 IgG antibody, in conjunction with chemotherapy treatment has become instrumental in improving HER2+ breast cancer survival, with patients that receive both treatments showing extended time to tumor progression and a reduced relative

risk of death by 20% (6). Despite this success, 70% of patients with HER2+ metastatic breast cancer show *de novo* (immediate) or acquired resistance to trastuzumab treatment (7). Patients with hormone-dependent tumors also show a greater chronic annual risk of relapse than non-hormone receptor tumors (4). Though combination treatment has greatly improved patient survival, metastases and recurrence still occur due to a subset of tumor cells evolving resistance to chemotherapy and/or hormone treatments.

Tumor dormancy

Tumor dormancy has become one tool in understanding both local and distant recurrence. Tumor cells that escape adjuvant chemotherapy and become dormant are distinct from primary tumor cells, in that they can remain asymptomatic and undetectable, but may eventually disseminate in a niche environment and establish a secondary tumor (2). Tumor dormancy has been observed clinically in breast cancer, prostate cancer, melanoma, and B-cell lymphoma (8–11). Once tumor cells have escaped from the primary tumor, they may enter the circulation for a period of time before disseminating at distant sites in the body. Circulating tumor cells (CTCs) have been found in breast cancer patients and were also found to persist during chemotherapy treatment, with CTC detection being linked to an increase in disease progression (12). Dormant tumor cells may also dissociate from the primary tumor prior to chemotherapy treatment. For example, disseminated tumor cells (DTCs) have been found in the bone marrow of prostate and breast cancer patients at the time of primary treatment, with no evidence of metastatic disease (13, 14). Such findings suggest that dormant tumor cells can escape from the primary tumor, even before the onset of treatment, change phenotype, and migrate to distant organs of the body, where they lie dormant and eventually establish secondary tumors.

Tumor dormancy is still poorly understood, however, there are thought to be 3 categories of tumor dormancy: cellular dormancy, angiogenic dormancy, and immune-mediated dormancy (15). Cellular dormancy is characterized by G0/G1 arrest, where cells enter a quiescent state due to external stress or selective pressure, whereas angiogenic dormancy is a balance of cell proliferation and cell death due to lack of proper nutrients reaching the tumor site. Immunogenic dormancy is characterized by equilibrium between cytotoxic killing of tumor cells, primarily mediated by CD8+ T lymphocytes, with tumor cell proliferation (16). These mechanisms are highly interconnected and can all be involved in the establishment and maintenance of dormancy. For example, tumor cells may be driven to quiescence (cellular dormancy) due to external stress of chemotherapy treatment (17). Other cells may maintain a reduced proliferative state, balanced with apoptosis (angiogenic dormancy), which allows them to evolve beneficial mutations to escape treatment or downregulate tumor-specific antigens. Lastly, once these dormant cells escape the primary tumor, the immune system can prevent recurrence by an effective anti-tumor response (immunogenic dormancy). Little is known about the molecular characteristics underlying tumor dormancy and there is a need to better understand how and why they are able to establish recurrence.

Immunogenic tumor dormancy requires the recognition of tumor cells by the immune system and subsequent anti-tumor response in order to keep transformed cells from developing into overt disease. Under the current model for immunogenic dormancy, dormant cells are thought to continually divide and subsequently be killed by CD8+ T lymphocytes. Because they remain in a proliferative state, such dormant cells can undergo selection. Dr. Schreiber was the first to propose the concept of immunoediting, in which tumor cells under immune surveillance undergo genomic alterations to escape from tumor-targeted immune cells (18). Tumor cells

escaping immune-surveillance and developing overt disease is defined as the 'elimination phase,' whereas tumor cells lying dormant and in check by the immune system is defined as the 'equilibrium phase' (19). Immunoediting involves genomic or epigenetic changes, such as loss of tumor antigens or antigen-presenting machinery, allowing for evasion of immune cells and establishment of disease (20). This process is also thought to be involved in the establishment of primary tumors, which begin as small neoplasms held in check by the immune system and eventually overwhelm the immune system and grow unchecked. In better understanding the mechanisms underlying dormancy, tumor-intrinsic pathways may be targeted to prevent induction of dormancy or maintain dormant tumor cells in the equilibrium phase, thus preventing escape and recurrence for life.

Chemotherapy-induced dormancy

Neo-adjuvant and adjuvant chemotherapies are standard of care treatments for detectable breast tumors. Chemotherapeutic agents induce apoptosis in most tumor cells, however, due to the heterogeneity of tumors, a small portion of cells can evade drug-induced apoptosis by entering a quiescent or growth reduced (indolent) state, with some eventually develop drug-resistance (21). Mellor and his group were able to show this phenomenon *in vitro*, by generating a multicellular dormant tumor spheroid model using human colon adenocarcinoma cells. Their spheroid dormant tumor cell model displayed marked decrease in Ki67 expression and increase in $p27^{kip1}$, a marker of quiescence. Their group showed that in comparison to several other drugs, doxorubicin showed significantly reduced potency in killing dormant tumor cells. Though doxorubicin (Adriamycin) is effective in killing most rapidly-dividing tumor cells, dormant cells

can enter a non-dividing or slow-dividing state, which renders such treatment ineffective in eliminating them.

Adriamycin (ADR) is a topoisomerase II inhibitor commonly used for neo-adjuvant and adjuvant breast cancer treatment. ADR acts in two ways to induce apoptosis in cancer cells: 1) Intercalation into DNA and disruption of topoisomerase-II-mediated DNA repair causing inhibition of growth and biosynthesis, and 2) generation of free radicals causing damage to cellular components (22). While ADR induces apoptosis in most tumor cells, a small portion of tumor cells that undergo selection and survive are resistant to apoptosis through induction of dormancy. In addition to induction of apoptosis, ADR treatment also contributes to the anti-tumor immune response. ADR-induced apoptosis in tumor cells has been found to cause immunomodulation through expression of markers associated with immunogenic cell death (ICD), such as calreticulin (CRT), heat shock protein 70 (HSP70), high mobility group box 1 (HMGB1) (23). A recent study demonstrated that upon Adriamycin treatment, malignant cells also produced type 1 interferons (IFNs) after the activation of Toll-like receptor 3 (TLR3) (24). Interestingly, tumors lacking TLR3 failed to respond to treatment. Through an autocrine signaling loop, type 1 IFNs trigger release of CXCL10, which acts as a chemoattractant for monocytes/macrophages, T cells, NK cells, and dendritic cells (DCs) (25). Such data suggests that in addition to apoptosis, immune-related pathways are activated upon Adriamycin treatment and such signaling is important in understanding induction of tumor dormancy.

Molecular mechanisms of dormancy

The changes that allow tumor cells to enter a dormant state, maintain a dormant state, escape immune surveillance, and relapse at distant sites years later remains enigmatic. A balance between growth and apoptotic signaling has been thought to play a role in dormancy, with a higher apoptotic to growth signaling ratio favoring dormancy and vice versa for recurrence (26). Depending on this ratio, dormant cells may either enter complete growth arrest ($Ki67^{-}$), referred to as quiescent dormancy, or maintain a slow proliferation ($Ki67^{+/low}$), referred to as indolent dormancy. Several apoptotic pathways have been implicated in dormant cell-signaling. The apoptotic-associated MAP kinase, p38, was found to be upregulated in dormant human ovarian cancer cells, causing activation of mitogen-activated protein kinase (MAPK) kinase 4/c-Jun NH2-terminal kinase (JNK)-activating kinase (collectively referred to as MKK4), which led to suppression of tumor growth and inhibition of tumor colony formation (27). Hickson and his group demonstrated that MKK4 activity in ovarian carcinoma cells is essential for metastasis suppression and the presence of MKK4 prolonged animal survival. A head and neck carcinoma model showed that disruption of the metastasis associated urokinase receptor (uPAR), which drives tumor growth in this model, led to activation of the p38 signaling pathway, driving cells to a dormant state (28). Furthermore, *in vivo* imaging in this model showed that dormancy resulted from complete inhibition of the growth factor signaling pathway, Raf-Mek-ERK, and induction of G0/G1 arrest. Such changes in growth and apoptotic signaling could be one way in which cells maintain a state of dormancy until they reach a favorable environment. If the activation of apoptotic pathways, such as JNK or p38, is too strong in tumor cells, it will lead to cell death instead of dormancy (29). Thus, the delicate balance of apoptotic and growth signaling that allows for dormancy, instead of apoptosis, might represent a survival mechanism evolved by

tumor cells to adapt and persist in stressful environments until they are eventually able to resume growth (30).

Signaling received from the tumor microenvironment (TME) can play an equally large role in prolonging dormancy. Patel *et al* found that CTCs expressing the chemokine receptors CXCR4 or CXCR7 were homed to the bone marrow due to CXCL12-expressing bone marrow stroma cells (31). These dormant cells also displayed unique gap junction intercellular communication with the bone marrow stroma which maintained DTCs in a dormant state, in which they are often found in the bone marrow. The bone marrow is also known to secrete factors known to drive quiescence, such as CXCR4, stem cell factor-1 (SDF-1) and angiopoietin (ANG1) (32). Such results suggest that dormant cells express chemokine receptors in order to home to certain secondary locations and are kept in a dormant state by interaction with their secondary TME.

External signaling can influence the balance in growth and apoptotic signaling, switching cells from a higher ratio of apoptotic signaling to a higher ratio of growth signaling and causing recurrence in the secondary site. For example, a recent study showed that inhibition of a growth pathway associated kinase, ERK, and p38 activation in prostate cancer cells (PCa) was caused by BMP7 (TGF-β family member) secretion in the bone marrow (33). Such signaling kept PCa DTCs in a dormant state in the bone marrow. When TGF-β receptor 1 or p38 were systemically inhibited in a head and neck squamous cell carcinoma model, DTCs in the bone marrow resumed proliferation and established recurrence (34). Similarly, in breast cancer patients, VCAM-1 expression in the bone marrow led to tumor-intrinsic activation of the NF-kB pathway in dormant DTCs, activating growth and survival signaling which led to recurrence (35). Such results suggest that though genetic and epigenetic changes in cell signaling may initially select

for tumor cells to undergo dormancy, the crosstalk with the new microenvironment can determine continued dormancy or recurrence.

Dormant tumor cells may also secrete factors that directly augment their growth, independent of the TME, through autocrine signaling loops. Dolle *et al* demonstrated that breast cancer cells secrete nerve growth factor (NGF) in order to promote proliferation, with tumor cell growth being strongly inhibited by NGF-neutralizing antibodies (36). Of note, NGF is not naturally expressed by normal breast epithelial cells. Recent studies also report the ability of drug-resistant tumor cells to acquire mitogenic signals from autocrine loops, which leads to cell proliferation and tumor recurrence (37). Such autonomous signaling could allow tumor cells to dictate their own proliferative state, either maintaining dormancy or initiating recurrence, independent from the TME.

Another possible mechanism involved in tumor dormancy is autophagy, an evolutionary conserved process of self-digestion found in both healthy and cancerous cells. The role of autophagy is still being debated, with some studies showing its benefit to tumor growth and others showing increased tumor cell death (38). Both apoptotic and growth signaling pathways rely on ubiquitin and degradation of proteins in order for proper signaling to occur, therefore autophagy can alter both types of signaling. There has been mounting evidence showing that chemotherapy, radiation, and endocrine therapy can induce autophagy in tumor cells (39). One study found that blockade of autophagy with chloroquine (CQ) enhanced the ability of chemotherapy treatment to induce tumor cell death in lymphoma cells (40). This is thought to be due, in part, to prevention of drug degradation by the tumor cell. Such results indicate blockade of autophagy during chemotherapy treatment as one method in which the efficacy of

conventional tumor therapies could be improved, allowing for increased apoptosis and fewer cells escaping treatment through drug-resistance and dormancy.

Inflammation and cancer

Inflammation has long been associated with tumor incidence and progression (41). Inflammation, or the body's natural response to pathogenic agents or insult, restores homeostasis to affected tissues. If such response becomes unregulated however, it can become chronic and induce malignant cell transformation in surrounding cells (42). One mechanism in which this occurs is through the recruitment of inflammatory cells to chronically inflamed tissues, which leads to the production of reactive oxygen species (ROS). ROS induce DNA damage in local tissues, which may eventually lead to transformation of healthy cells. In addition to ROS production, several inflammatory mediators have been linked to cancer incidence and progression, such as TNF-α, IL-6 and TGF-β (34, 43, 44). One study found that long term users of aspirin and nonsteroidal anti-inflammatory drugs (NSAIDS) have a 40-50% reduced chance of developing colon cancer (45). It is also well documented that chronic inflammation by human papilloma virus or hepatitis B and C can lead to cervical or hepatocellular carcinoma (46). Though there is mounting evidence supporting chronic inflammation's role in tumor incidence, inflammation's role in tumorigenesis does not end there.

Inflammatory chemokines and cytokines are most often associated with immune cell signaling, however, such inflammatory regulators are also produced by tumor cells (47). Early in tumor initiation, many tumor types produce T_H1 cytokines (IL-1, TNF-α and IL-6) to create a pro-inflammatory microenvironment, which ultimately leads to neovascularization and rapid tumor growth (48–50). This acute inflammatory signal is also received by immune cells, which

flock to the tumor site and initiate an anti-tumor response (51). Tumor cells upregulate immunosuppressive molecules such as PD-L1 and FAS, causing T cells anergy or death (52). In addition to T cell anergy, tumor cells have been found to produce GM-CSF and prostaglandins E_2 (PGE_2), causing expansion of myeloid-derived suppressor cells (MSDSs), which further promote tumor growth (53). IL-1β and TNF-α production in the TME have been shown to switch macrophages to an M2-phenotype, tumor-associated macrophages (TAMs), which tolerate and foster tumor growth instead of attacking it (54). Tumor cells not only hijack these factors to augment inflammatory cell migration and activation, but also to promote their own growth in the TME. Perhaps the best example of this phenomenon is in melanoma cells, which have been shown to secrete CXCL1, CXCL2, CXCL3, and IL-8 to exert autocrine control over cell proliferation and metastasis (55). Tumor cells can autonomously utilize a myriad of inflammatory mediators in creating a pro-inflammatory TME in order to induce tolerance or differentiation of pro-tumor immune cells and regulate their own growth and metastases.

The inflammatory mechanisms related to cancer can be described in the crosstalk between two pathways: 1) The intrinsic pathway, which is driven by genetic and epigenetic changes and oncogene expression in tumor cells, and 2) the extrinsic pathway which is driven by environmental factors, such as the TME or immune response (53). Oncogene expression alone in tumor cells can result in the production of inflammatory cytokines. Sparmann and his group showed that oncogenic Ras expression caused upregulation of IL-8 in Hela cells, which resulted in the recruitment of immune cells and angiogenesis in their murine xenograft model (56). Oncogenic Ras has also been shown to cause production of IL-1β, IL-6 and IL-8 in ovarian epithelial cells (57). In conjunction with intrinsic pathways, extrinsic pathways also induce inflammatory signaling in tumor cells. For example, when subject to hypoxic conditions, tumor

cells will adapt through the activation of hypoxia-inducible transcription factor (HIF)-1. HIF-1 activation leads to production of genes associated with angiogenesis (VEGF-A), anaerobic metabolism (GLUT1) and invasiveness (MMPs) through the subsequent activation of NF-κB or STAT3 (58). NF-κB or STAT3 initiate further downstream signaling perpetuating inflammation in the TME.

NF-κB signaling in cancer and dormancy

NF-κB has been nicknamed the master regulator of stress and consists of five family members: RelA (p65), RelB, c-Rel, NF-κB1 (p50), and NF-κB2 (p52) (59). All members of the NF-κB family form active homodimers/heterodimers and bind to enhancer regions of DNA that regulate the transcription of genes related to a wide variety of functions (60). NF-κB proteins are held in the cytoplasm, inhibited by IκB, until a signal is received by the cell (60). In the classical pathway, signals received from lipopolysaccharides (LPS), TNF-α and IL-1β cause phosphorylation of IκB, allowing for NF-κB translocation to the nucleus and transcription of target genes related to inflammation (61). Conversely, in the alternative pathway, B-cell activation factor (BAFFR), lymphotoxin β-receptor (LTβR), CD40 and nuclear factor kappa B (RANK) initiate signaling which leads to ubiquitination of p100 and subsequent proteasomal processing to p52-RelB heterodimers can then activate transcription of target genes related to immune cell differentiation and maturation (62). These pathways can overlap both in signaling and in target genes, with the main difference between them being the signals which activate them. Several other kinases are involved in both types of signaling, which result in a complex signaling cascade that allows cells to respond quickly to different stress situations. In addition to

the production of inflammatory cytokines, such as TNF-α, IL-1, and IL-6, NF-κB signaling also controls cell growth and apoptosis (63, 64).

Alterations in tumor-intrinsic NF-κB signaling is a recent discovery that has prompted many new questions in cancer research. NF-κB's role in tumor initiation and progression is dichotomous: tumor-intrinsic NF-κB signaling is required for proper immune response via acute inflammation leading to anti-tumor activity, however, constitutive NF-κB signaling causes chronic inflammation which can have pro-tumorigenic effects (65). Huber and his group demonstrated that NF-κB signaling is essential for EMT and subsequent metastases in human breast cancer cells (66). Interestingly, they also showed that inhibition of NF-κB in mesenchymal cells caused reversion back to an epithelial phenotype, suggesting that NF-κB is not only essential for EMT, but also involved in maintenance of this metastatic state. Furthermore, NF-κB signaling in tumor cells has been shown to cause upregulation of VEGF and subsequent vascularization, which leads to rapid tumor growth (67). Tumor cells control NF-κB signaling by either evolving mutations in NF-κB (or developing oncogenic mutations which upregulate it) or secreting inflammatory cytokines in the microenvironment (68). Such evidence suggests that tumor-intrinsic NF-κB signaling promotes metastasis and survival in several tumor types and such signaling could be involved in the survival of dormant tumor cells.

The NF-κB p65/p50 heterodimer primarily controls the transcription of pro-inflammatory cytokines via the classical pathway (69). Though all the functions of every heterodimer is not known, NF-κB p65 knockdown in human macrophages from inflammatory bowel disease patients significantly reduced the production of inflammatory cytokines, affirming that this subunit is a key player in the transcription of inflammatory mediators (70). NF-κB p65 is unique from other NF-κB family members in that it can be acetylated at many different sites, suggesting

that the transcriptional activity of NF-κB p65 is fine-tuned and allows for target-gene specificity and timing of gene expression, rather than just acting in an on or off state (69). The customization of NF-κB p65 transcription regulation allows for a time-specific production of particular inflammatory cytokines depending on the signals received by the cell.

Due to the regulatory customization of NF-κB p65 and large amount of target genes related to inflammation, it is no surprise that tumor cells have hijacked this transcription factor for their advantage. Amplification of NF-κB p65 due to point mutations was recently found in human B-cell lymphoma, owing to its oncogenic potential (71). NF-κB p65 can also crosstalk with other apoptotic and cell cycle-related transcription factors, such as p53 tumor suppressor and STAT3 (72). STAT3-mediated acetylation causes increased NF-κB p65 activity, which results in secretion of inflammatory cytokines such as IL-6 (72). STAT3 activation in cancer induces anti-apoptotic genes such as Bcl-2 and Bcl-X (73). Interestingly, NF-κB p65 has also been shown to inhibit p53 transactivation, and vice versa, in mice (74). Such crosstalk allows NF-κB to control a wide range of pathways related to growth and apoptosis, and for this reason, there is a need to better understand the role of NF-κB in tumor dormancy and recurrence.

The aim of this study was to evaluate the role of tumor-intrinsic signaling in ADR-induced tumor dormancy and recurrence. Microarray and gene analysis data allowed us to pinpoint inflammatory signaling in both dormancy and recurrence. We hypothesized that knockdown of NF-κB p65 in mouse mammary carcinoma cells (MMC) would cause a delay in tumor relapse, due to inhibition of NF-κB survival signaling during ADR treatment, thus preventing cells from entering a dormant state and becoming resistant to ADR-induced apoptosis. Our results suggest that NF-κB p65 is involved in drug-resistance and dormancy

signaling pathways, however, further studies are required to confirm its precise role in dormancy and recurrence.

Materials and Methods

Mouse model

All animal experiments were performed with FVBN202 transgenic mice (The Jackson Laboratory; Bar Harbor, ME) between 8 and 12 weeks of age. These mice overexpress rat neu transgene under the regulation of the mouse mammary tumor virus promoter (75). These studies have been reviewed and approved by the Institutional Animal Care and Use Committee at Virginia Commonwealth University.

Tumor cell lines

The neu-overexpressing mouse mammary carcinoma (MMC) cell line was established from a spontaneous mammary tumor harvested from a FVBN202 mouse (76). Tumor cells were maintained in RPMI 1640 without L-glutamine (L-glut) (RPMI-L-glut) prior to being switched to RPMI 1640 supplemented with L-glut (2µM) (RPMI+L-glut). Both were supplemented with 10% fetal bovine serum (FBS) and cells were kept at 37ºC with 5% CO_2. Cells were routinely passaged when needed with 0.25% Trypsin or 10mM Ethylenediaminetetracetic acid (EDTA) solution (Quality Biologicals Inc., Gaithersburg, MD).

Trypan Blue Exclusion

Cell count and viability were determined with Trypan Blue exclusion. Cells were detached with 10mM EDTA for 5 minutes at 37ºC with 5% CO_2, neutralized with equal volume RPMI supplemented with 10% FBS, and centrifuged at 1200 rpm for 6-8 minutes at 4ºC. The supernatant was discarded and pellet was resuspended in fresh RPMI. Cells were diluted either 1:20 or 1:4, depending on the size of the pellet, with 0.4% trypan blue solution (Sigma-Aldrich, St. Louis, MO). The solution was added to the hemocytometer (Hycor, Garden Grove, CA) and white, trypan blue-negative cells were counted as viable while blue, trypan blue-positive cells

were counted as dead. Cells/mL was determined by dividing the 9-grid count by 9 and multiplying by the dilution factor and 10^4.

Antibodies

Western blot antibodies: purified anti-NF-κB p65 (Biolegend), anti-GAPDH produced in rabbit (Sigma), and Amersham ECL Rabbit IgG, HRP-linked F(ab')$_2$ fragment (from donkey)(GE Healthcare Bio Sciences, Pittsburgh, PA).

All flow cytometry antibodies were purchased from Biolegend unless otherwise stated: anti-Ki67 PE (16A8), Annexin V FITC, anti-CD45 BV785 (30-F11), anti-c-ErbB2/c-Neu (B104-1-1) (Millipore), Biotin Mouse Anti-Mouse H-2D[q]/H-2L[q] (KH117) (BD Biosciences), anti-B220 AF594 (RAE-6B2), anti-CD11c PE (N418), anti-CD11b APC (M1/70), anti-Gr1 FITC (RB6-8C5), andti-CD3 BUV395 (17A2) (BD Biosciences), anti-CD4 BUV737 (GK1.5) (BD Biosciences), anti-CD8 BV711 (53-6.7), anti-CD49b APC/Cy7 DX5), anti-CD274 (B7-H1, PD-L1) (10F.9G2), anti-IgG AF594 (Poly4053) and Streptavidin PE. Anti-mouse CD16/32 (93) blocking antibody was used only with *in vivo* samples.

Establishment of dormancy *in vitro*

MMC were seeded at 5 x 10^6 cells/flask 24 hours prior to experiment. On the day of treatment, cells were seeded at 3 x 10^6 cells/flask and incubated at 37°C with 5% CO_2 for 4 hours to adhere. Once adherent, cells were treated with and without 10μM CQ (Sigma-Aldrich, St. Louis, MO) and incubated for 3 hours in the dark at 37ºC with 5% CO_2. 1μM of Adriamycin (ADR) (Sigma-Aldrich, St. Louis, MO) was added directly to the flasks and cells were incubated for 2 additional hours, with CQ being in culture for a total of 5 hours. Cells were washed with sterile 1X PBS and fresh medium was added to the culture. Treatment was repeated for three consecutive days and cells were left in culture for varying times, depending on the experiment.

Medium was changed as needed and floater cells were counted via Trypan Blue exclusion after being collected by centrifugation.

RNA extraction and Microarray Analysis

RNA extraction and microarray analysis was performed as previously described by our group (77). Tumor cells were lysed with TRIzol reagent (Thermo Fisher Scientific, Waltham, MA) and RNA was isolated on days 0 (untreated), 4, 21 and 42 after the treatments. RNA quality control was conducted to ensure RNA integrity and all RNA samples surpassed quality standards. *JustRMA* software with *Biobase* and *Affy* packages were run in the R environment to normalize the microarray data. Microsoft excel was used in order to generate Venn Diagrams in order to isolate probe sets that contained genes uniquely upregulated or downregulated in dormancy and relapse.

Ingenuity Pathway Analysis (IPA)

Each experimental group of differentially expressed genes, containing Affymetrix probe set IDs and fold changes with a p-value less than 0.001, were uploaded into IPA (Ingenuity Systems, http://www.ingenuity.com) and analyzed with the Mouse Genome 430A 2.0 Array platform as a reference model. Core Analysis function was performed to analyze pathways affected by changes in gene expression. Diseases and Functions were analyzed from probe sets unique to dormancy or relapse isolated from Venn Diagram analysis with p-values less than 0.01. Canonical Pathways and Upstream Regulators were analyzed from all significantly upregulated or downregulated probe sets from each group (without Venn Diagram Analysis) and were filtered based on a p-value less than 0.01 and z-score greater than the absolute value of 2.0. The IPA p-value is based upon the likelihood that expression of various genes within a pathway will be upregulated or downregulated by chance and have no effect on that pathway. Z-score predicts

which pathways or regulators are likely activated or inhibited based upon the upregulation or downregulation of genes in the data set.

Multiplex cytokine array

Cytokine array was performed by the Cytokine Core Laboratory (University of Maryland, Baltimore, MD) on a Luminex Multianalyte system. Samples were prepared by detaching cells at 1 or 3 weeks with 10mM EDTA and reseeding 1 x 10^6 cells/mL/well in a 6-well plate. After 4 hours when cells had adhered, the medium was replaced to remove dead cells and debris. Cells were incubated for an additional 24 hours at 37ºC with 5% CO_2. Supernatant from each group was collected and immediately frozen at -80°C. Samples were shipped through FedEx overnight on dry ice.

NF-κB p65 shRNA transduction

The shNF-κB p65 cell line was produced by transducing MMC with NF-κB p65 shRNA Lentiviral Particles (Santa Cruz Biotech., San Diego, CA). The particles contain 4 target-specific constructs that encode 19-25 nt (plus hairpin) shRNA designed to knock down gene expression. Varying multiplicity of infections (MOIs) and concentrations of Polybrene (Santa Cruz., San Diego, CA) were used in order to optimize transduction. 24 hours prior to transduction, MMC were seeded at 50% confluency in a 12-well plate in 1mL of complete medium (RPMI 1640, 10% FBS, L-glutamine (2μM), 100U/mL penicillin, and 100 μg/mL Streptomycin). The following day, the medium was removed and replaced with complete medium containing 4 μg/mL or 8 μg/mL of Polybrene. The lentiviral particles were thawed and added directly to the cultures at an MOI of 3 or 7. Cells were incubated overnight at 37ºC with 5% CO_2. The following day, the medium was removed and replaced with fresh complete medium. After cells were allowed to grow for two days, 5 μg/ml of Puromycin dihydrochloride (Santa Cruz Biotech.,

San Diego, CA) was added to select for those cells which had been successfully transduced. SCR-MMC were transduced with control shRNA Lentiviral Particles-A (Santa Cruz Biotech., San Diego, CA), which encode a scrambled shRNA sequence that does not lead to degradation of any known mRNA, alongside NF-κB p65 transduction. Transduced cells were kept in Puromycin-selection RPMI for all downstream experiments.

NF-κB p65 CRISPR-Cas9 transfection

CRISPR-Cas9 gene editing technology was used to create a complete knockout of NF-κB p65. The CRISPR-Cas9 plasmid was purchased from Sigma's cloning service which provided a single vector containing the Cas9 protein expression cassette and guide RNA (gRNA) to target the second exon site within the RELA (p65) gene. 0.3×10^6 MMC cells/mL/well were seeded in a 6 well plate in complete medium 24 hours prior to transfection. The following day, 2mL of fresh complete medium was added along with the CRISPR plasmid and jetPrime reagent (Polyplus, New York, NY) in a 1:2 ratio. Medium was replaced after 4 hours and cells were left in culture for 48 hours prior to FACS selection. An empty GFP control plasmid was used alongside CRISPR plasmid transfection to serve as a GFP control.

Preparation of cell extract and western blot analysis

Successful knock down of NF-κB p65 was determined via western blot analysis. Cells were detached with 10mM EDTA and centrifuged at 1200 rpm for 8 minutes at 4ºC. The pellet was suspended in 500 µL of 1X PBS (PBS), transferred to a 1.5mL microcentrifuge tube, and washed twice with PBS. Residual PBS was decanted and cells were resuspended in 500µL of pre-cooled radioimmunoprecipitation assay (RIPA) buffer (Thermo Fisher Scientific, Waltham, MA), with appropriate amounts of Halt protease and phosphatase inhibitor cocktail (Thermo Fisher Scientific, Waltham, MA) and PMSF (Sigma-Aldrich, St. Louis, MO) freshly added. Cells

were incubated for 30 minutes on ice and passed through a 26g needle in order to further disrupt the cell membrane during lysis. Samples were then centrifuged at 12,000 rpm for 15 min at 4ºC. Supernatant was collected and protein concentration was measured using Pierce BCA Protein Assay Kit (Thermo Fisher Scientific, Waltham, MA), following manufacturer specifications. 10µg of protein sample was run on an SDS-PAGE gel and transferred to nitrocellulose paper overnight at 4ºC. Western blot was performed using anti-NF-κB p65 or anti-GAPDH, followed by rabbit IgG Horseradish Peroxidase (HRP)-linked secondary antibody for detection.

Establishment of tumor dormancy *in vivo*

FVBN202 mice were inoculated with 3 million shNF-κB p65 or SCR-MMC in sterile 1X PBS subcutaneously in the mammary fat pad. Mice were weighed and tumor size was monitored by digital caliper twice weekly. Tumor size was calculated by V[volume] = (L[length] $_x$ W[width]^2)/2. Mice were injected with 9mg/kg of ADR intravenously every 3 days when tumor size reached between 400 and 800mm^3. Mice were euthanized when tumor size had reached 2000mm^3 and tumors were collected in complete medium for further analysis.

***In vitro* expansion of splenocytes**

Reprogramming of tumor-sensitized immune cells was performed as previously described by our group (78). FVBN202 mice were inoculated with 3 million shNF-κB p65 or SCR-MMC in the mammary fat pad and growth was monitored by digital caliper. Spleens were harvested when tumor size was between 1000mm^3 and 2000mm^3. Splenocytes were cultured in complete medium and were stimulated with 1µM of Bryostatin 1 (Sigma, Saint Louis, MO), 1µM of Ionomycin (Calbiochem, San Diego, CA), and 80 U/mL/10^6 cells of recombinant human IL-2 (Peprotech, Rocky Hill, NJ) for 16-18 hours. Bryostatin 1 and Ionomycin mimic intracellular signaling that results in activation of recently sensitized T cells by activating protein

kinase C and mobilizing intracellular Ca^{2+} (78). Lymphocytes were then washed three times and cultured in complete medium with recombinant murine IL-7 and IL-15 (20ng/mL of each, Peprotech). After 24 hours, 20 U/mL of IL-2 was added to the culture and the following day cells were washed and cultured with 40 U/mL of IL-2. After 48 hours, cells were washed again and 40 U/mL of fresh IL-2 was added. 24 hours later, lymphocytes were washed again and cultured with 40 U/mL of fresh IL-2. Lymphocytes were harvested 24 hours later on the 6^{th} day and were used for cytotoxicity experiments.

Cytotoxicity Assay

Expanded T-cells from shNF-κB p65 or SCR-MMC-inoculated mice were co-cultured with MMC at a ratio of 10:1 in complete medium supplemented with 40U/mL of IL-2 for 2 days as previously described by our group (78). Supernatant was collected and combined with adherent cells, that were detached with 10mM EDTA, and cells were analyzed with flow cytometry.

Flow cytometry

FVS and Ki67 staining

Ki67 expression was determined as previously described by our group (17). Cells were fixed with 70% ethanol and stained with anti-Ki67 for 30 minutes at room temperature. Prior to fixation, cells were also stained with Fixable Viability Stain (FVS) (BD Biosciences, Franklin Lakes, NJ) for 20 minutes at room temperature. Cells were washed twice with FACS buffer (1X PBS, 10% FBS, 0.1% sodium azide) prior to acquisition.

Annexin V and PI staining

In order to determine the level of early apoptosis, late apoptosis and necrosis for cytotoxicity assay, cells were detached with 10mM EDTA and washed twice with 1X Annexin

Buffer (BD Biosciences, San Jose. CA) at 1200 rpm for 8 minutes at 4ºC in round bottom polystyrene tubes. Cells were incubated with anti-Annexin V for 15 minutes, then propidium iodide (PI) (Sigma, Saint Louis, MO) and 400µL of 1X Annexin buffer was added immediately prior to sample acquisition.

Multi-color cell surface staining

A multi-color staining and flow cytometry analyses were performed as previously described by our group (17), with some modifications. Infiltrating lymphocytes were analyzed by multi-color staining of resected tumors. Animals were euthanized when tumors reached >1000mm^3 and tumors were surgically cut from the animal in an aseptic environment. The tumors were minced into smaller pieces using scissors and forceps. A plunger from a disposable 5mL syringe was used to mechanically disaggregate the tumor against a secured filter. Complete medium was used to wash any remaining cells through the filter. Cells were washed with ice-cold FACS buffer at 1200 rpm for 10 minutes at 4°C and counted via Trypan blue exclusion. 1 x 10^6 cells were placed in sample and single-color control tubes and washed once more with FACS buffer. Cells were blocked with anti-mouse CD16/32 antibody for 20 minutes on ice, followed by two washes. Cells were then stained with anti-c-ErbB2/c-Neu primary antibody or anti- H-2D[q]/H-2L[q] (MHCI) and incubated for 20 minutes on ice. Following 2 washes with FACS buffer at 1200 rpm for 10 minutes at 4°C, cells were stained with anti-CD45, anti-B220, anti-CD11c, anti-CD11b, anti-Gr, anti-CD3, anti-CD4, anti-CD8, anti-CD49b, anti-PD-L1, anti-IgG secondary or Streptavidin for 20 minutes on ice. Cells were washed twice and data acquisition was performed immediately after staining. Neu, PD-L1 and MHCI expression was determined *in vitro* following the same staining protocol.

Data acquisition was performed on a Beckon-Dickenson FACS Fortessa X-20 flow cytometer. Each sample contains 10,000-20,000 events and all data was analyzed using FCS express software 5 (De Novo Software, Loa Angeles, CA). Appropriate compensation was performed and all gating was determined using autofluorescence and single-color controls.

FACS GFP sorting

Transfection efficiency for the CRISPR-Cas9 p65 and GFP control plasmid was analyzed by GFP expression level. Cells were detached with 10uM EDTA and washed with complete medium at 1200 rpm for 8 minutes at 4°C. Each sample was sorted into GFP-low and GFP-intermediate populations using a Beckon-Dickenson FACS Aria III cell sorter in sterile conditions. GFP-high expressing cells were excluded from the NF-κB $p65^{-/-}$ sorted cells due to increased probability of Cas9 off-target effects.

Statistical analysis

Data was summarized by mean and standard error of the mean (SEM) with differences between groups being illustrated with graphical data presented as mean ± SEM. Statistical comparisons were made using a one-tailed, type 2 Student *t* test and a p-value <0.05 was considered significant.

Results

Chloroquine prolongs ADR-induced tumor dormancy in MMC

Based on evidence suggesting that CQ enhances the effects of chemotherapy treatment, we investigated the effects of CQ on ADR-induced dormancy by using our previously described *in vitro* model for tumor dormancy. MMC cultured with RPMI-L-glut exhibit ADR-induced tumor dormancy by week 3 and relapse by week 6 after treatment (n=3). Relapse was determined by adherent cell-count, which showed a significant ($p=0.04$) increase at week 6 compared to week 3 (Fig. 1A). MMC treated with CQ 2 hours prior to ADR treatment did not relapse by week 6, showing no significant changes in adherent cell count, and therefore representing maintenance of dormancy. Both groups maintained proliferative capacity throughout dormancy, yet observable adherent cell number did not change. This proliferative capacity was confirmed by Ki67 staining at each time point, with a $Ki67^{+/low}$ population remaining during dormancy (Fig. 1B), as well as production of floater cells throughout the 3 or 6-week cultures (Fig. 1C).

We sought to determine if the small population of viable floater cells would remain viable if cultured separately, which could provide a useful in *vitro* model for dormant CTCs. Floater cells were collected at various time points throughout the experiment and cultured for several days (n=1). Regardless of the time collected, all floater cells died after 4 days of culture (Fig. 1D).

In order to determine whether dormant cells have a distinct gene expression signature compared to relapsed MMC, microarray analysis was performed for each experimental group

Figure 1. ADR induces tumor dormancy in MMC, *in vitro.*
MMC tumor cells were treated with 3 daily doses of ADR (1uM for 2 hs), with one group receiving CQ (10uM for 3 hs) immediately prior to ADR treatment. Both groups remained untreated for 3 weeks and 6 weeks, *in vitro*. A) Adherent cells were counted using trypan blue exclusion 3 and 6 weeks after treatment. B) MMC+ADR were analyzed for Ki67 expression on FVS negative viable cells (gating not shown). C) Floater cells were collected whenever culture medium was replaced and cell number and viability was assessed via trypan blue exclusion. D) Floater cells were cultured separately for 2-3 days each time they were collected, and assessed for viability 2-4 days later. Data represent 3 independent experiments and mean ± SEM.

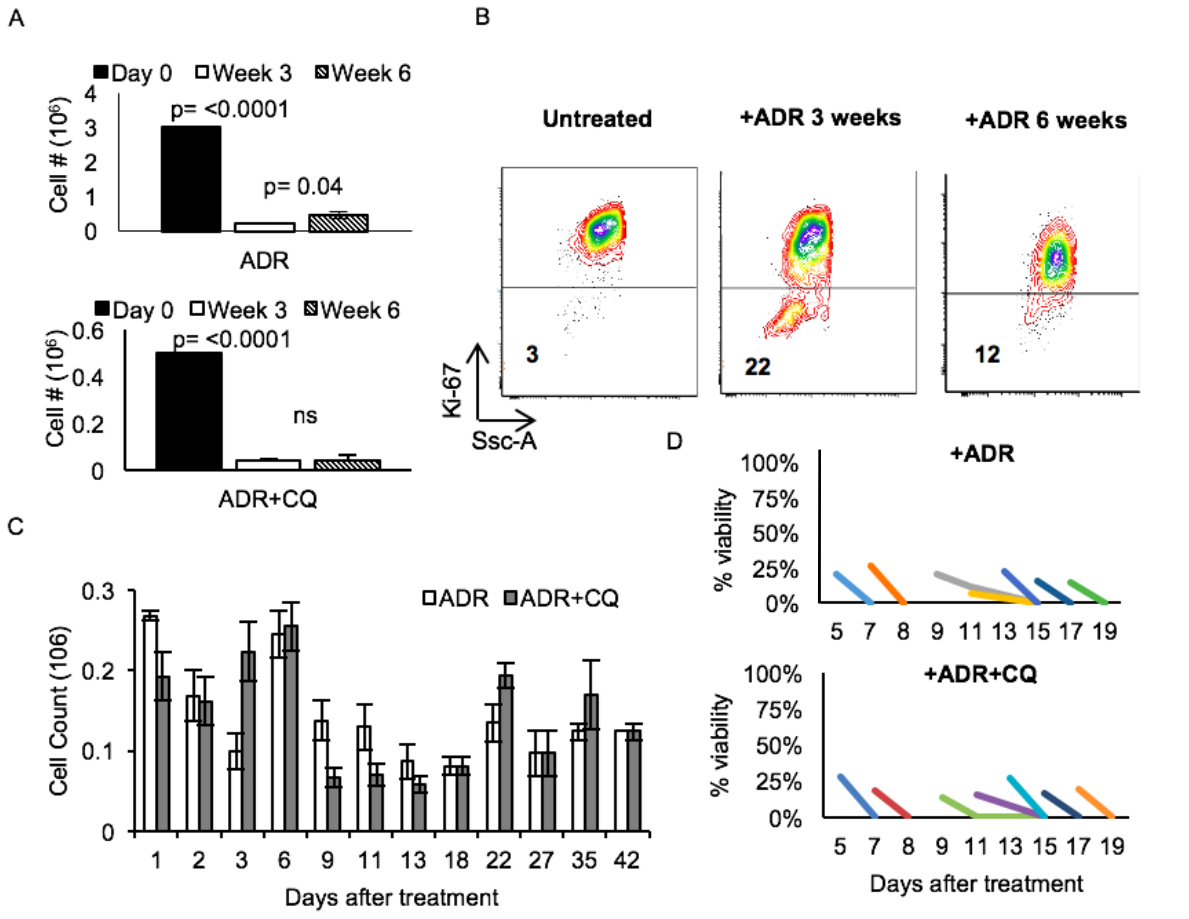

(n=3). Untreated MMC and MMC+CQ day 4 were included as controls. Fold change in gene expression for each group was determined by comparison with untreated MMC control. Unsupervised cluster analysis shows close clustering among the ADR+CQ groups at both the 3-week and 6-week time points, representing maintenance of dormancy. Conversely, the ADR groups at the 3-week and 6-week time points, representing dormancy and relapse, clustered apart from one another (Fig. 2).

Dormant and relapsing MMC show unique inflammatory signature

We then sought to determine the gene profile unique to each experimental group. Venn diagram analysis showed 239 genes unique to dormancy when both dormant groups were compared (MMC+ADR week 3 vs MMC+ADR+CQ week 3) (Fig. 3A upper panel). 682 genes unique to prolonged dormancy were found by comparing the fold changes of the relapsing group (MMC+ADR week 6) with the prolonged dormancy group (MMC+ADR+CQ week 6) (Fig. 3A lower panel). The prolonged dormancy group (MMC+ADR+CQ week 6) and relapsing group (MMC+ADR week 6) shared 882 common probe sets. Each probe set group was then analyzed for disease function by Ingenuity Pathway Analysis (IPA). The 239 genes involved in dormancy showed a z-score increase in disease states related to acute inflammation, while the 682 genes unique to relapse showed predicted activation in disease states related to chronic inflammation (Fig. 3B). The 882 genes shared by both week 6 groups, one relapsing and the other dormant, showed predicted activation of both chronic and acute disease states.

In order to pinpoint pathways and proteins involved in inflammation, all probe sets that showed a significant upregulation or downregulation for each experimental group were uploaded to IPA and comparison analysis on canonical pathways and upstream regulators was performed (Fig. 3C). Most notably, RelA (NF-κB p65) showed predicted activation (z-score=2.6) only in

Figure 2. Dormant MMC exhibit unique gene signature compared to relapsing MMC. Unsupervised cluster analysis was performed on microarray probe set expression values. There is close clustering of experimental groups MMC+ADR+CQ at weeks 3 and 6 during the establishment and maintenance of tumor dormancy. However, tumor cells that enter the dormant state at week 3 and resumed a sluggish proliferation at week 6 (MMC+ADR week 3 and week 6) were clustered apart from each other. Control groups (MMC and MMC+CQ) were clustered together.

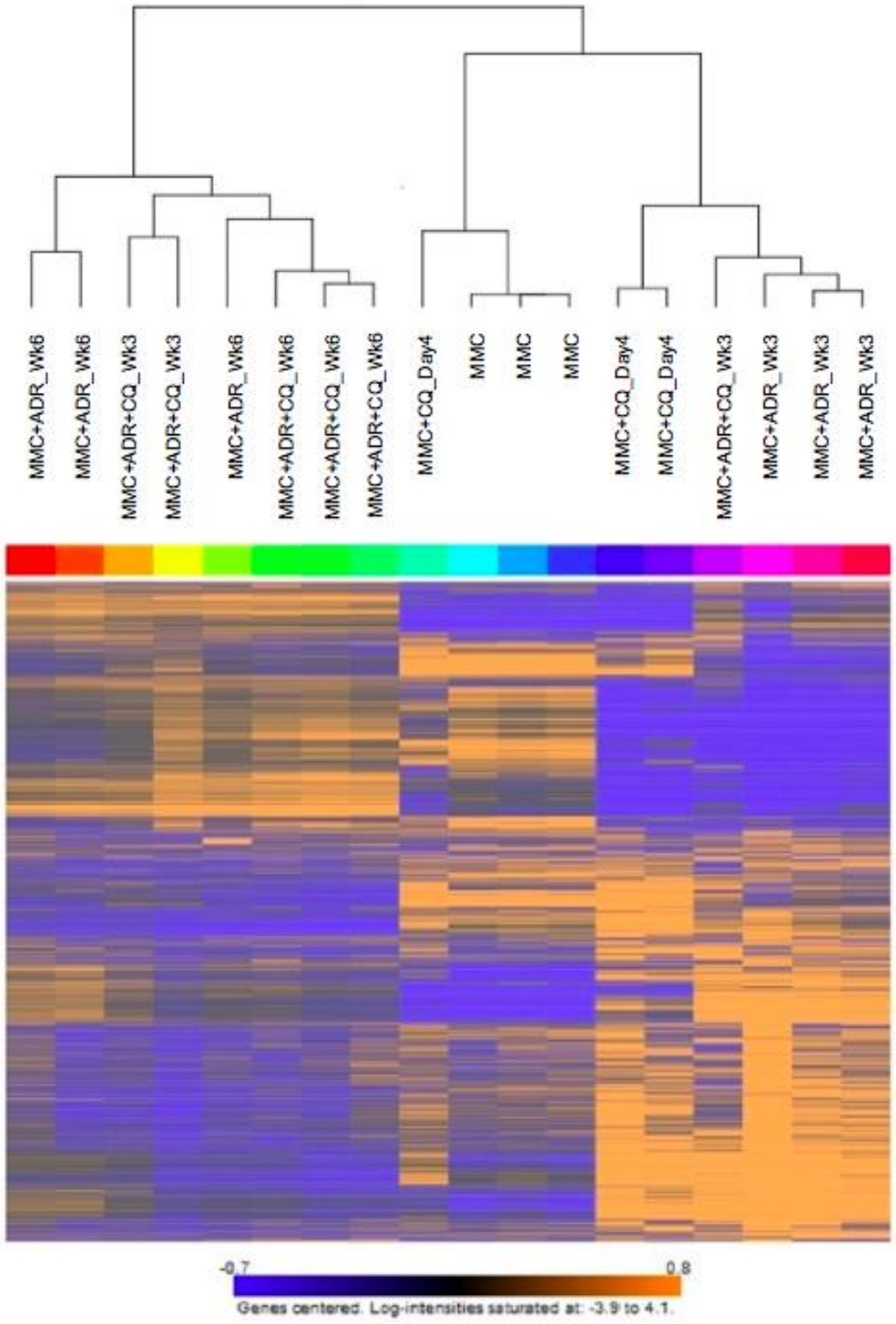

Figure 3. Inflammatory gene signature during dormancy and relapse.
A) Venn Diagram analysis isolated 239 probe sets unique to dormancy when comparing both dormant groups (upper panel) and 682 unique probe sets unique to relapse when both week 6 groups were compared (lower panel). 882 probe sets were shared between the MMC+ADR week 6 relapsing group and the MMC+ADR+CQ week 6 prolonged dormancy group. Venn diagrams were generated from microarray fold-change expression data. Fold change was calculated by comparing each group to untreated MMC expression. B) Ingenuity Pathway Analysis (IPA) reveals genes among 239 shared probe sets involved in maintenance of dormancy shows predicted activation of disease states related to acute inflammation, 682 probe sets unique to relapse show predicated activation of disease states related to acute inflammation, and 882 shared probe sets involved in both maintenance and escape from dormancy show predicated activation of disease states related to acute and chronic inflammation. C) IPA comparison analysis shows predicted activation and inhibition of canonical pathways and upstream regulators based on z-score. RelA showed a significant (z-score=2.6) predicted activation in the dormant group (MMC+ADR week 3). All significant ($p<0.0001$) fold change expression data for each experimental group was included in comparison analysis.

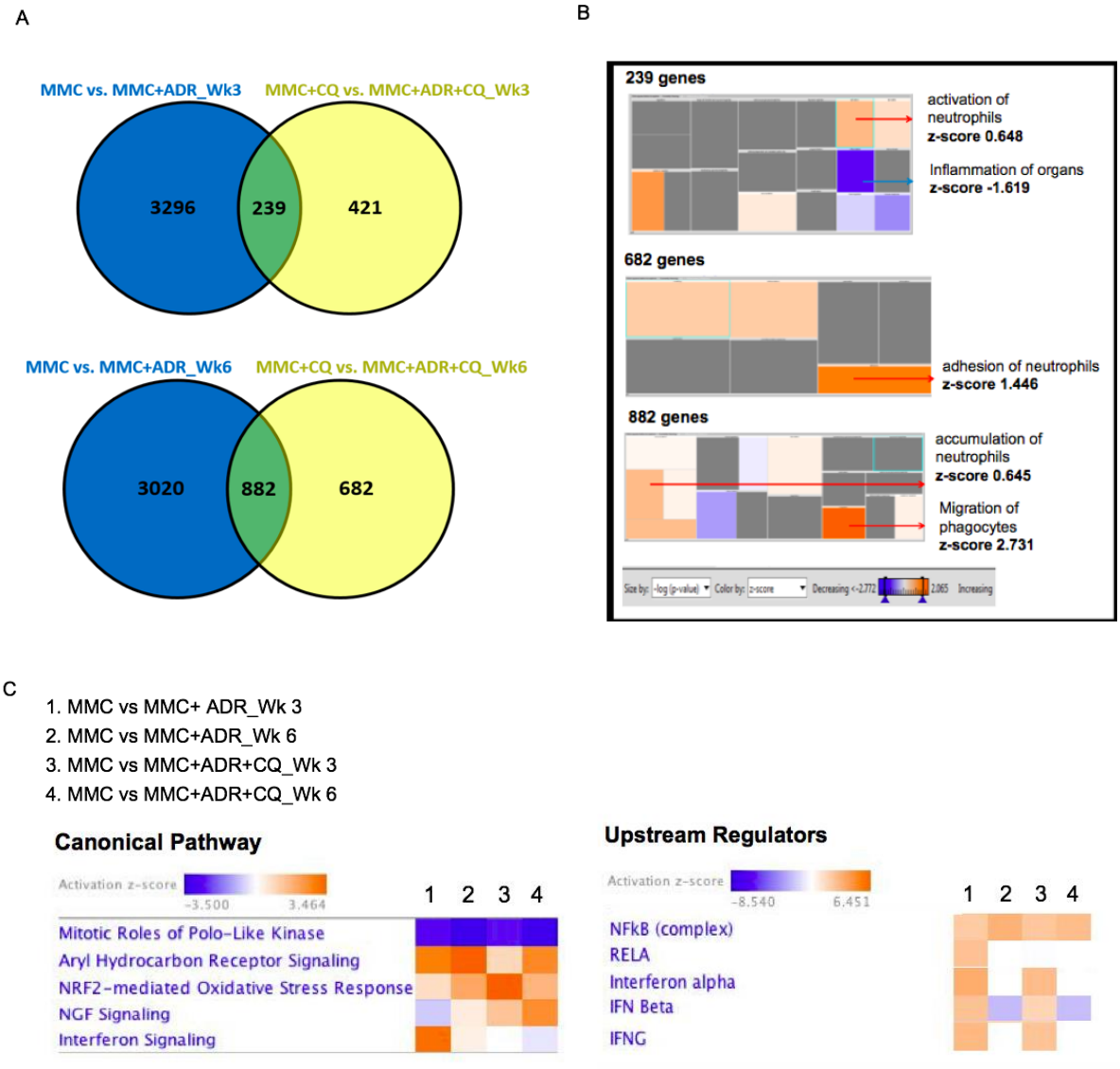

the MMC+ADR week 3 dormant group. NF-κB (complex) showed predicted activation in all groups, however, the highest z-scores were in the MMC+ADR week 6 relapsing group and MMC+ADR+CQ week 6 prolonged dormancy group (z-score=3.26 and 2.79). Type 1 interferons (alpha and beta) showed predicated activation in the MMC+ADR week 3 dormant group (z-score= 3.5 and 2.6) and the MMC+ADR+CQ week 3 dormant group (z-score=2.5 and 1.77). Interferon gamma (IFNG) also showed predicted activation in both dormancy groups (z-score=2.9 and 2.5). Interferon Signaling was shown to be highly activated (z-score=3.16) only in the MMC+ADR week 3 dormant group.

In order to determine whether the predicted activation of RelA led to the secretion of inflammatory cytokines during dormancy (preceding relapse) a multiplex cytokine array was performed on the supernatant from the MMC+ADR week 3 group. Cytokines probes were chosen by analysis of robust multi-array average (RMA) expression data for inflammatory cytokines that showed unique upregulation during dormancy. Choice of cytokine was also limited based on market availability. The protein concentration corroborated mRNA expression level from the microarray data for each cytokine, except RANTES, which shows a decrease in protein expression (Fig. 4).

L-glutamine-addiction increases the rate of relapse in MMC

Following the previous results, MMC were cultured exclusively with RPMI+L-glut in order to better replicate *in vivo* conditions, with L-glut being present in biological systems. After several months of exposure to L-glut, cells were removed from RPMI+L-glut and grown in RPMI-L-glut. After 2 days, cell number and viability significantly dropped (Fig. 5A), with all cells eventually succumbing to death (data not shown). L-glut-addicted MMC were then treated

Figure 4. Secretion of inflammatory cytokines during dormancy, *in vitro*.
MMC were treated 3 times daily with ADR (1uM for 2 hs) and left in culture for 3 weeks. Cells were then detached and re-seeded in a 6-well plate alongside untreated MMC. After 24 hours of culture, supernatant from each well was collected. RMA (log_2) value from microarray data and concentration (pg/mL) of each cytokine are compared side-by-side. Targets were chosen based on microarray data and commercial availability.

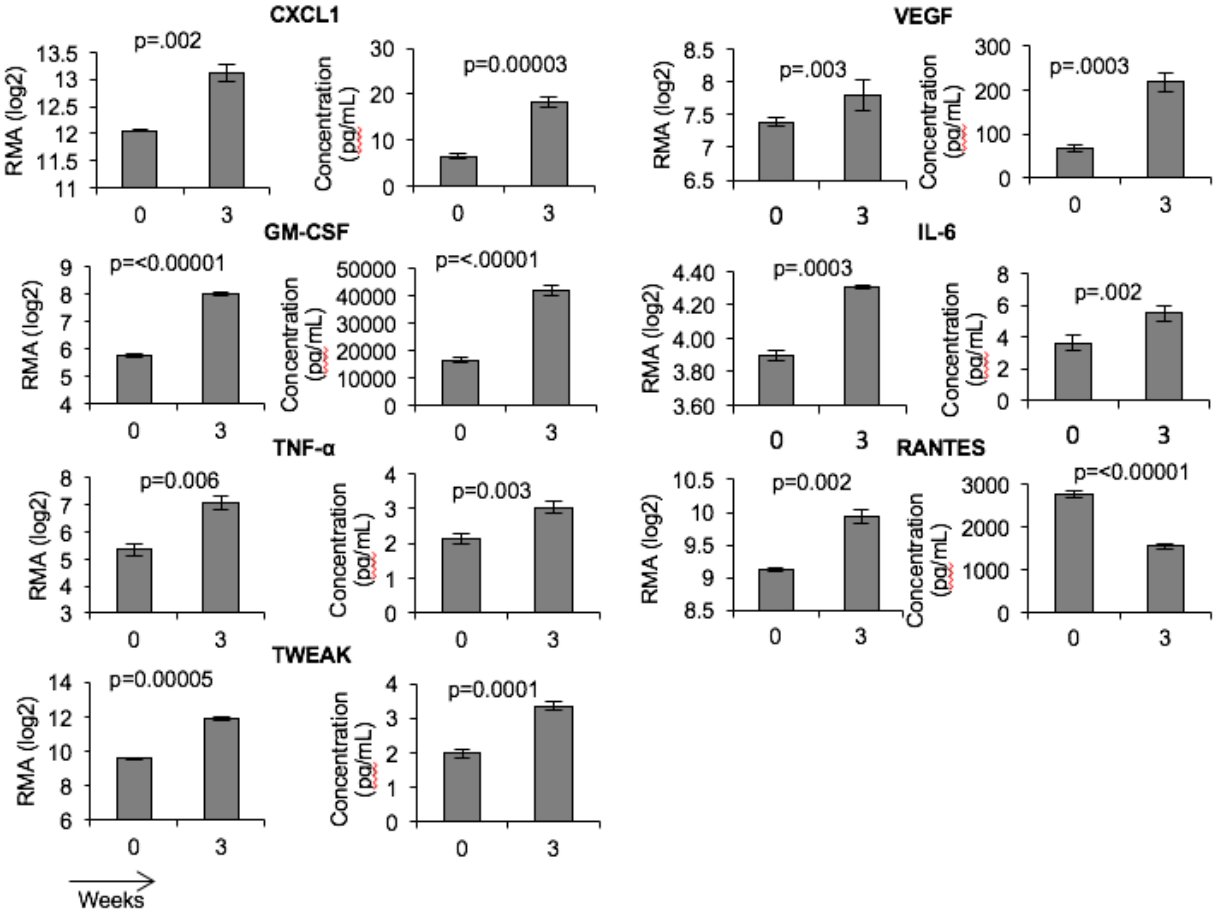

Figure 5. L-glutamine addiction in MMC results in increased rate-of-relapse.
A) MMC was cultured and passaged in RPMI+L-glut for several months. Cells were then either left in culture with RPMI+L-glut or cultured with RPMI-L-glut for 2 days. Cells were counted and assessed for viability via trypan blue exclusion B) L-glut addicted MMC were treated with 3 daily doses of ADR (1uM for 2 hs), with one group receiving CQ (10uM for 3 hs) immediately prior to ADR treatment. Both groups remained untreated for 3 weeks. Cells were detached and counted via trypan blue exclusion. Data represent 3 independent experiments and mean ± SEM.

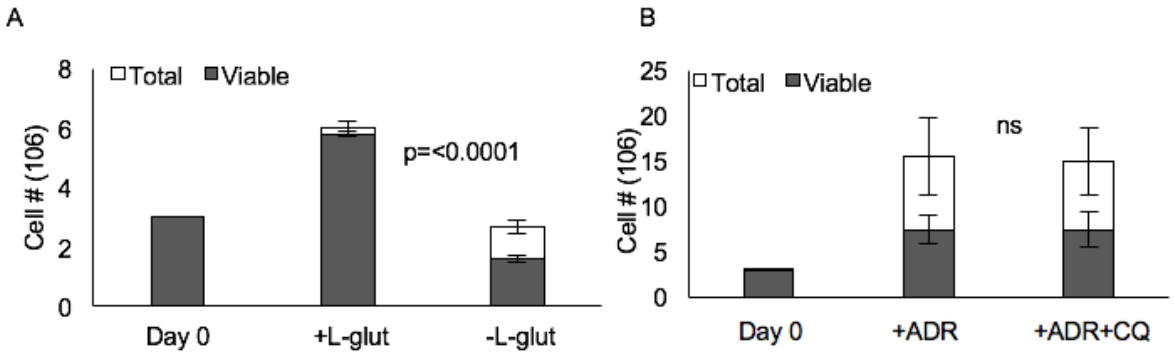

with ADR+/-CQ, as described above, and cells were observed for an increase in adherent cell number. After 3 weeks, both experimental groups had undergone drastic relapse compared to non-addicted MMC (Fig. 1A), with no statistical differences between either experimental group (Fig. 5B)

ADR-treated shNF-κB p65 exhibit reduced growth and a reduced rate of relapse *in vitro* and *in vivo.*

Though CQ is most noted for its effects on blocking autophagy, unpublished data from our lab showed that autophagy protein 5 (ATG5) shRNA knockdown MMC resulted in a higher rate of relapse compared to control MMC. Therefore, transient blockade of autophagy alone during drug treatment could not be the cause for the delay in relapse of that group. In addition to blockade of autophagy, CQ has been shown to inhibit NF-κB through blockade of IkB degradation (79). Because of such findings, and IPA results suggesting unique NF-κB p65 signaling pathways during dormancy, we created an shRNA knockdown of NF-κB p65 in L-glut-addicted MMC in order to determine if prolonged dormancy in CQ-treated MMC was due to NF-κB inhibition. MMC were transduced using lentiviral particles containing NF-κB p65 shRNA (shNF-κB p65) or SCR shRNA (SCR-MMC) and remaining cells were subject to puromycin selection and western blot analysis (Fig. 6A).

shNF-κB p65 and SCR-MMC were then treated with ADR as described above. Based on increased relapse rate in L-glut-addicted MMC, the week 1 time point represents dormancy, whereas the week 3-time point represents relapse (Fig. 6B). Both groups entered dormancy, with overall adherent cell number decreasing as expected. However, while both groups increased in cell number by week 3, shNF-κB p65 had significantly ($p=0.04$, $p=0.03$) fewer adherent cells at

Figure 6. NF-κB p65 knockdown in MMC reduces the rate of relapse, *in vitro*.
A) Western Blot analysis shows knockdown of NF-κB p65 shRNA-transduced MMC, after puromycin selection, alongside control MMC and SCR-MMC. GAPDH was used as the housekeeping control. B) shNF-κB p65 and SCR-MMC were treated 3 times daily with ADR (1uM for 2 hrs) and left in culture for 1 or 3 weeks. Cells were detached and assessed for cell number and viability via trypan blue exclusion. C) shNF-κB p65 and SCR-MMC were seeded at 3 x 10^6 cells/flask and left in culture for 48 hours. Cells were detached and counted via trypan blue exclusion. Data represent 3 independent experiments and mean ± SEM.

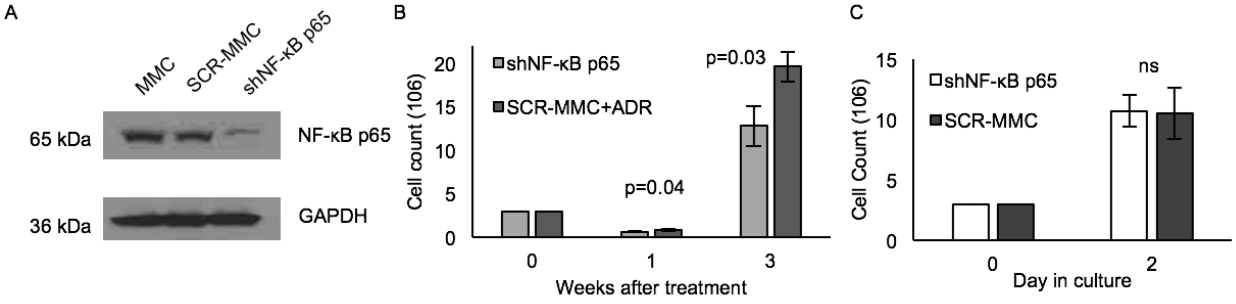

both time points when compared to the SCR-MMC group. In order to confirm that this change was due to sensitivity to ADR and not differences in baseline proliferation rate, shNF-κB p65 and SCR-MMC were seeded at 3 million per flask (n=3). After 48 hours in culture, adherent cell count was determined via trypan blue with no significant changes in in cell number (Fig. 6C).

Growth rate and response to ADR treatment was determined *in vivo* by subcutaneously injecting FVBN202 mice with 3 million shNF-κB p65 or SCR-MMC in the mammary fat pad (n=3). Tumor size initially showed no significant changes in growth between both groups (Fig. 7A). However, when animals were treated intravenously with ADR (9mg/kg) every 3 days beginning on day 36, shNF-κB p65 tumors showed significantly (p=0.01) reduced growth compared to SCR-MMC tumors by day 54. A fraction of tumor cells were then cultured *in vitro* for 2 weeks upon resection from the animal in order to confirm stable shRNA knockdown of NF-κB p65. Western blot analysis of each tumor shows maintained knock down of NF-κB p65 to varying degrees (Fig. 7B).

shNF-κB p65 showed increased neu expression in response to ADR treatment *in vitro* and *in vivo*

We then sought to determine if tumor-intrinsic NF-κB p65 signaling pathways had any effect on immunomodulation of ADR-treated MMC by analyzing neu, PD-L1, and MHCI expression. shNF-κB p65 and SCR-MMC were treated with ADR as described above (n=3). On day 7 post treatment, cells were detached and analyzed for neu, PD-L1, and MHCI expression by flow cytometry. Mean florescence intensity (MFI) showed significant upregulation of neu expression in ADR-treated cells when compared to untreated control in both groups (p=0.0007 and p=0.01) (Fig. 8A). However, shNF-κB p65 displayed significantly higher upregulation when

Figure 7. shNF-κB p65 tumors show reduced growth in response to ADR treatment, *in vivo*. A) 3 x 10^6 shNF-κB p65 or SCR-MMC were injected subcutaneously into the mammary fat pad of FVBN202 naïve mice (n=3). Mice were treated every 3 days with 9mg/kg of ADR beginning 36 days post challenge, when tumors has reached ~800mm^3, and euthanized on day 54 when tumors had reached greater than 2000mm^3. Tumors were measured twice weekly by digital caliper. B) Remaining tumor samples were cultured for two weeks and western blot analysis was performed separately for each animal.

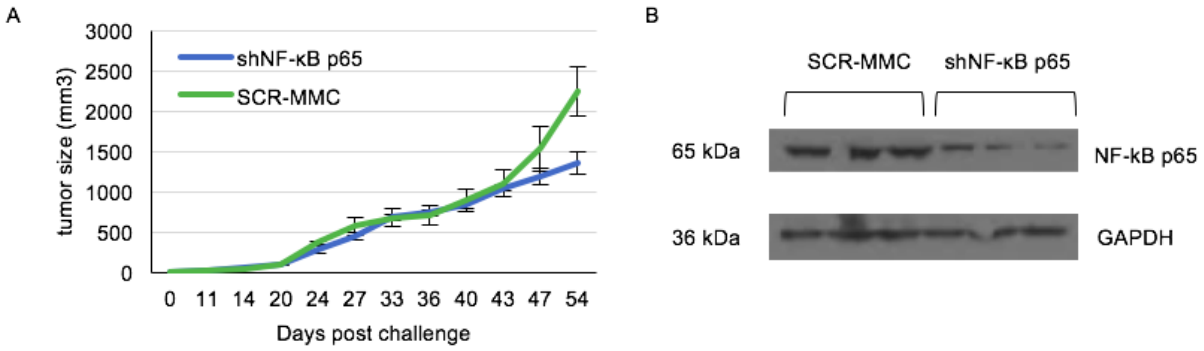

Figure 8. shNF-κB p65 show higher upregulation of neu in response to ADR treatment. A) shNF-κB p65 and SCR-MMC were treated 3 times daily with ADR (1uM for 2 hrs) and left in culture for 1 week. Neu, PD-L1, and MHC1 expression was determined by MFI. B) 3 x 10^6 shNF-κB p65 or SCR-MMC were injected subcutaneously into the mammary fat pad of FVBN202 naïve mice. Mice were treated every 3 days with 9mg/kg ADR 36 days post challenge, when tumors has reached ~800mm^3, and euthanized on day 54 when tumors had reached greater than 2000mm^3. Control mice were injected with 5 x 10^6 of each and euthanized when tumors had reached >800mm^3. Tumors were resected from mice and measured for neu expression by flow cytometry. MFI was determined by gating on CD45-/neu+ cells only.

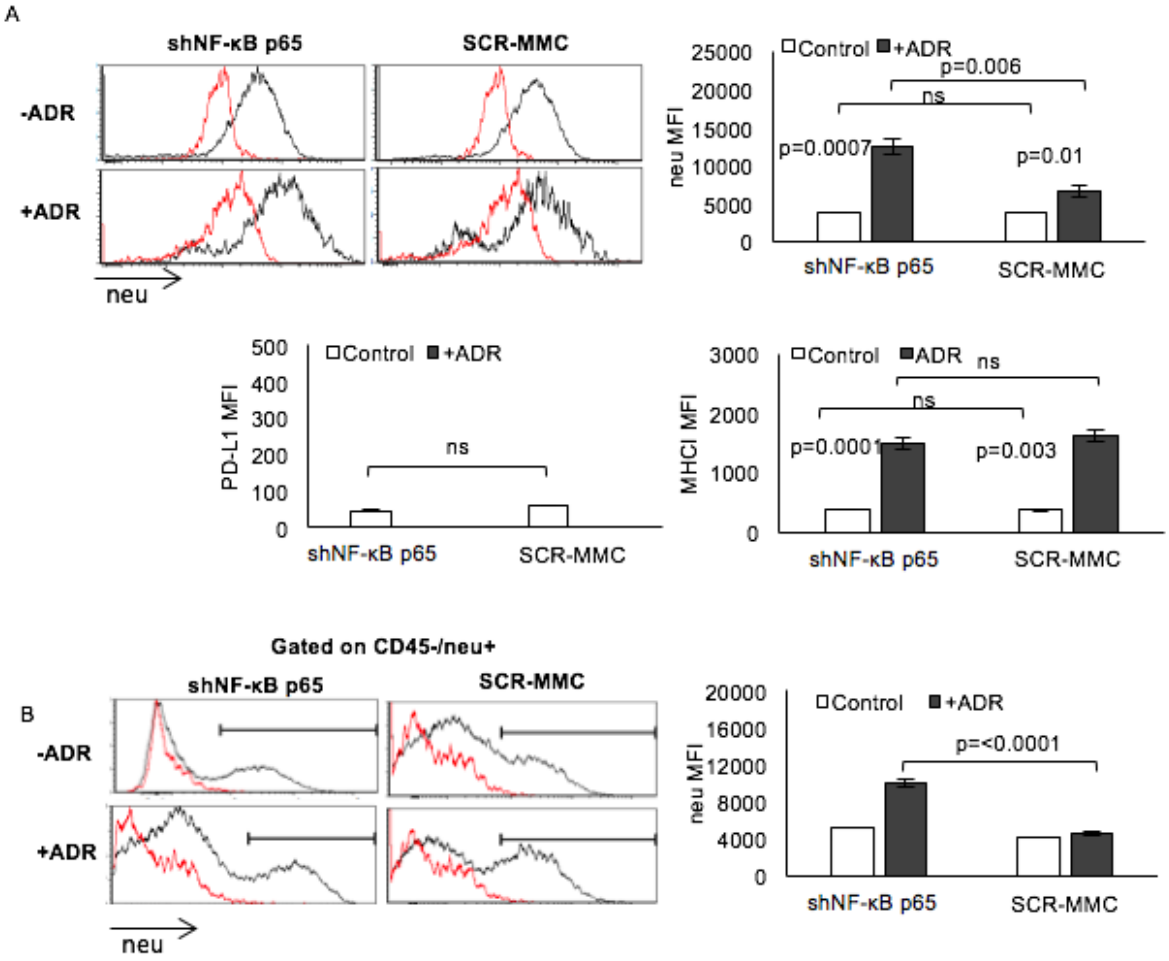

compared to SCR-MMC (p=0.006). Both shNF-κB p65 and SCR-MMC showed no increase in PD-L1 MFI after ADR treatment, and while MHCI MFI did increase upon ADR treatment, there were no significant differences between shNF-κB p65 and SCR-MMC. Due to significant changes in neu expression between ADR-treated shNF-κB p65 and SCR-MMC, we chose to focus solely on neu expression for *in vivo* staining. Tumors resected from shNF-κB p65 or SCR-MMC-inoculated mice treated with ADR (n=3) (described above), along with control mice (n=1), were stained for neu expression following the same protocol. Neu upregulation showed the same trend *in vivo*, with increased neu MFI in ADR-treated mice but a larger increase in the shNF-κB p65 compared to SCR-MMC tumors (p=<0.0001) (Fig. 8B).

shNF-κB p65 show augmented tumor-infiltrate and reduced anti-tumor response

We then sought to determine if tumor-intrinsic NF-κB p65 signaling pathways had an effect on infiltration of CD45+ immune cells or the particular immune-cell type. shNF-κB p65 or SCR-MMC tumors resected from ADR-treated mice (n=3) were stained with CD45 and compared with that of non-treated mice (n=1) (Fig. 9A). Additional staining for CD11b, GR1, CD3, CD4, CD8, B220, CD49b was performed only on non-treated mice from each group. Log_2 frequency ratios showed the fold change increase or decrease in percentages of each cell type and was calculated by comparing the log_2 ratio of shNF-κB p65 sample percentages to those of SCR-MMC (80). While total CD45+ infiltrate showed no significant differences between the ADR-treated groups, the non-treated shNF-κB p65 tumor showed a decrease in CD3+CD8+ cytotoxic T cells and an increase in CD11b+GR1+ monocytes/macrophages compared to the SCR-MMC tumor.

In order to investigate the role of NF-κB p65 in the anti-tumor immune response, splenocytes were collected from ADR-treated mice which had been inoculated with either shNF-

Figure 9. shNF-κB p65 tumors display alteration of tumor infiltrate *in vivo* and T cell activation *ex vivo*.
A) 3 x 10^6 shNF-κB p65 or SCR-MMC were injected subcutaneously into the mammary fat pad of FVBN202 naïve mice (n=3). Mice were treated every 3 days with 9mg/kg ADR 36 days post challenge when tumors has reached ~800mm^3. Mice were euthanized on day 56 when tumors had reached greater than 2000mm^3. Control mice were injected with 5 x 10^6 shNF-κB p65 or SCR-MMC and euthanized when tumor reached ~800mm^3. Tumors were resected from ADR-treated mice and control mice and analyzed for CD45 expression (left panel). Control mice tumors were analyzed for CD45, B220, CD3, CD8, CD4, CD11b, CD11c, GR1 and CD49b expression and compared by mean log_2 frequency ratio (right panel). B) MMC were cultured with expanded T cells from splenocytes of untreated shNF-κB p65 or SCR-MMC inoculated mice and cultured for two days in the presence of IL-2. *Ex vivo* expansion of T cells prior to co-culture shows poor expansion of splenocytes from shNF-κB p65 mice (bottom left). Both adherent and floater cells were counted and stained with Annexin V and PI to determine viability. Representative dot plots show cells in early/late apoptosis and necrosis (top). Total apoptotic includes early apoptotic, late apoptotic and necrotic cells (bottom right).

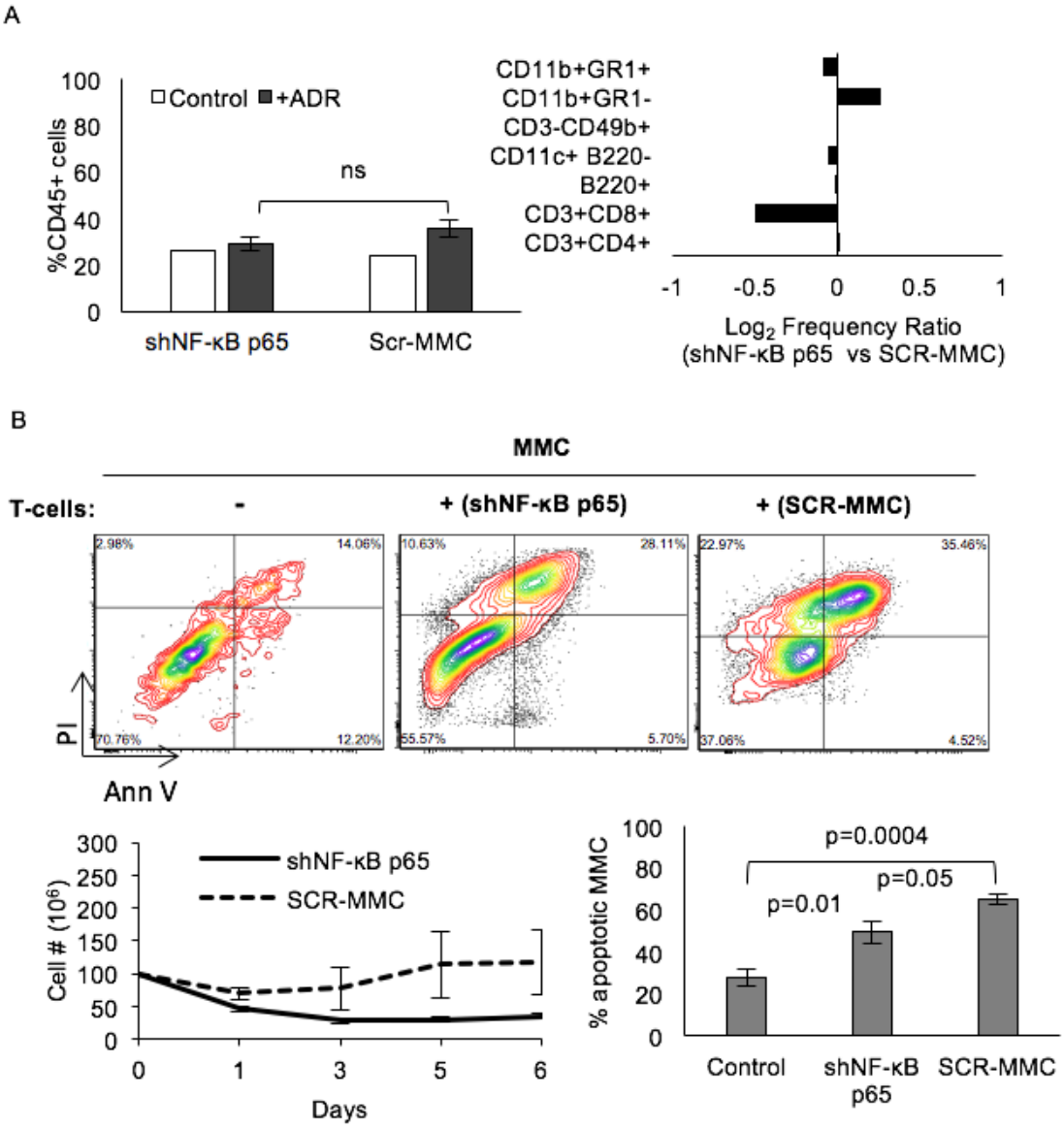

κB p65 or SCR-MMC tumors (n=3). Reprogramming of tumor-sensitized immune cells was done *ex vivo*, as previously described by our group (78). Splenocytes from shNF-κB p65 tumors showed significant (p=0.05) reduction in expansion, based on final cell count, compared with those from SCR-MMC tumor mice (Fig. 9B). MMC remained sensitive to tumor-reactive lymphocytes taken from SCR-MMC tumor mice, with 65% apoptosis of target MMC. However, tumor-reactive lymphocytes isolated from shNF-κB p65 tumor mice showed reduced cytotoxic killing of MMC, with 49% apoptosis (p=0.05).

CRISPR-Cas9 complete knockdown of NF-κB p65 in MMC

In order to confirm shRNA results, we created a complete knockout cell line using the CRISPR-Cas9 gene editing system. MMC were transfected with a CRISPR-Cas9, GFP-tagged plasmid, which included gRNA targeting the second exon sequence in the murine RELA gene. A control GFP plasmid was used as the negative control. Cells were sorted with FACS 48 hours post-transfection and measured for transfecting efficiency by GFP expression (Fig. 10A). GFP-MMC control cells were sorted into two populations based on low and int/high GFP expression, whereas the NF-κB $p65^{-/-}$ were sorted intro two populations, but cells expressing high GFP were excluded due to the increased probability of off-target gene editing effects. Complete knockdown of each transfected group was confirmed with western blot analysis, with both GFP-expressing populations showing complete knockdown of NF-κB p65 (Fig. 10B). Non-treated proliferation data matched that of shNF-κB p65, showing no significant changes in cell number from the control group (Fig. 10C). NF-κB $p65^{-/-}$ and GFP-MMC were treated with ADR as described above. NF-κB $p65^{-/-}$ showed a reduction in cell number 5 days after ADR treatment, with overall adherent cell-count being significantly (p=0.02) less than the GFP-MMC control (Fig. 10D).

Figure 10. CRISPR-Cas9 knockout of NF-κB p65 in MMC
A) MMC transfected with CRISPR-Cas9-GFP-NF-κB p65 plasmid were assessed for GFP expression by FACS sorting. Each sample was sorted into two groups, based on level of GFP expression, and cultured separately for further analysis. B) Western blot analysis was performed for each sample to determine NF-κB p65 expression. C) NF-κB $p65^{-/-}$ and GFP-MMC were seeded at 3 x 10^6 cells/flask and left in culture for 48 hours to compare proliferation rate. D) Both groups were also treated 3 times daily with ADR (1uM for 2 hrs) and then left in culture for 5 days. Cells were detached and assessed for cell number and viability via trypan blue exclusion. Data represent 3 independent experiments and mean ± SEM.

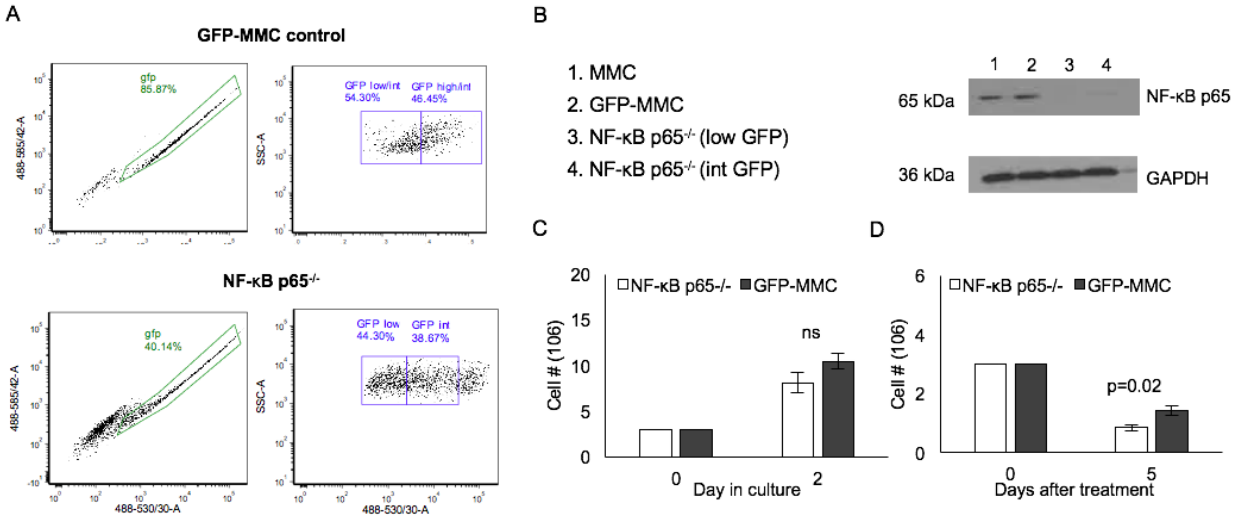

Discussion

The role of host-driven inflammation in tumor initiation has become better understood in recent years. However, the contribution of tumor-intrinsic inflammatory pathways in tumors, particularly in regards to tumor dormancy and recurrence, is poorly understood. We sought to study this phenomena by using our *in vitro* model of tumor dormancy, which allowed for isolation of tumor signaling with no extrinsic influence from the TME or immune system. While ADR-induced NF-κB pathways were found to be involved in tumor dormancy and relapse, ADR-induced NF-κB p65 activity was specifically associated with relapse. Upon finding that CQ prolonged dormancy and delayed relapse *in vitro*, further gene array analysis implicated differences in inflammatory signaling pathways, with NF-κB p65 in particular showing predicted activation in the ADR-treated dormant group that eventually relapsed. Activation of NF-κB p65 was associated with significant increases in the production of pro-inflammatory cytokines (e.g. TNF-α, IL-6, and GM-SCF) during ADR-induced dormancy, which suggests that cytokine production preceding relapse allows for constitutive activation of NF-κB during dormancy. shRNA knockdown of NF-κB p65 resulted in fewer dormant cells one week after treatment and a delay in relapse. Mice inoculated with shNF-κB p65 showed no changes in tumor growth initially, but upon ADR treatment, showed significantly slowed growth compared to SCR-MMC tumors. We also created a complete knockout cell line of NF-κB p65 using the CRISPR-Cas9 gene editing tool, which corroborated shRNA *in vitro* results. Additionally, we demonstrated that ADR-induced NF-κB p65 activity reduces the immunomodulatory effects of ADR, through inhibition of neu upregulation. shNF-κB p65 was more efficient in upregulating neu upon ADR treatment both *in vitro* and *in vivo*. Lastly, ADR-induced NF-κB p65 activity allows for CD8+ T

cell infiltration and an effective anti-tumor response. shNF-κB p65 tumors showed fewer CD8+ T cell and an increase in CD11b+GR1- monocytes/macrophages compared to SCR-MMC control tumors. T cells from animals with shNF-κB p65 tumors showed reduced expansion and potency in cytotoxic killing of MMC, *ex vivo*. Taken together, our data suggests that while tumor-intrinsic NF-κB signaling facilitates dormancy and relapse, it is also required for proper immune infiltration leading to an effective anti-tumor response.

Our current understanding of drug-induced dormancy is that tumor cells undergo epigenetic alterations upon ADR treatment and a fraction of cells able to evolve an optimal ratio of apoptotic to growth signaling will evade drug treatment through induction of dormancy. CQ, an anti-malarial drug, is most recognized in cancer research for its anti-autophagy effects in tumor cells (81). As a weak base, it accumulates in acidic organelles of cells, such as late endosomes and lysosomes, where it prevents fusion events and degradation of lysosomal cargo (82). Interestingly, additional data from our lab showed that ATG5 knockdown (autophagy deficient MMC) showed an increased rate of relapse upon ADR treatment, rather than the delayed relapse found in MMC treated with CQ. Such results suggest that the prolonged relapse in MMC treated with ADR+CQ could not have been entirely due to transient blockade of autophagy during drug treatment. Many survival pathways, such as NF-κB, rely on ubiquitination and degradation of enzymes in order to initiate a proper signaling cascade, with one study finding that CQ blocked NF-κB by inhibiting degradation of IκB (79). Microarray and IPA analysis from ADR and CQ-treated MMC showed predicted NF-κB p65 activation in the MMC+ADR dormant group, but not in the MMC+ADR+CQ group. This data suggests that NF-κB p65 signaling pathways after ADR treatment allows for induction of dormancy that eventually leads to relapse.

Interestingly, the CQ-causing delay in relapse was not seen in ADR-treated L-glut-addicted MMC. We chose to add L-glut in order to better replicate *in vivo* conditions in culture. However, when treated with ADR and ADR+CQ, both groups underwent drastic relapse by week 3, with no significant differences in cell number. Glutamine (GLN) is the most abundant free amino acid in the body, and cancer cells have been shown to heavily depend on GLN for growth and proliferation (83). The benefit of GLN to cancer cells has long been hypothesized to be due to GLN providing a carbon and nitrogen source by conversion of GLN into L-glut and ammonia (84). Recent studies suggest that GLN may also provide cells with acid resistance through enzymatic deamination, particularly *in vitro* (85). Such data suggest that the blockade effects of CQ were no longer sufficient in delaying relapse when cells received a growth advantage from L-glut addiction.

Our data suggests that NF-κB p65 activation during ADR treatment provides MMC with a tumor-intrinsic survival mechanism to escape from ADR-induced apoptosis through induction of dormancy, which supports similar findings in the field. For example, treatment with panobinostat and bortezomib, drugs that inhibit AKT and NF-κB signaling, in conjunction with ADR, resulted in apoptosis of leukemia cells, which had become resistant to ADR apoptosis through induction of dormancy (86). Another study found that treatment with the NF-κB inhibitor DHMEQ (dehydroxymethlypoxyquinomicin), in combination with cytotoxic therapeutics, resulted in significant reversal of drug-resistance and subsequent tumor cell death (87). Our findings support such data, with shNF-κB p65 having fewer cells one week after ADR treatment and slower proliferation rate upon relapse at three weeks, *in vitro*. shNF-κB p65 tumors also showed significant reduction in tumor growth upon ADR treatment, further confirming its role in

resistance to ADR-induced apoptosis. Western blot data of these tumors showed varying degrees of NF-κB p65 knockdown, which could have been due to fibroblast contamination *in vitro*.

The production of inflammatory cytokines by MMC during ADR-induced dormancy *in vitro* suggest that dormant MMC promote constitutive activation of NF-κB p65, rather than having direct mutations in NF-κB which leads to its upregulation. Additionally, oncogenic mutations in NF-κB have only been observed in B-cell lymphomas and direct mutations in NF-κB genes in solid tumors are rare (88). Nonetheless, they do occur, with one study revealing mutations in NF-κB p50 in human breast cancers (89). Further gene array studies could determine if oncogenic mutations in NF-κB signaling genes have occurred in our cell line and their contribution to these findings.

The cytokines produced by dormant cells can also give us insight into other signaling pathways working in conjunction with NF-κB to induce dormancy. CXCL1 traditionally acts as a neutrophil attractant, though it has been shown to be secreted by human melanoma cells and promotes pathogenesis through mitogenic signaling (90, 91). TNF-α is well known to activate a multitude of pathways, such as NF-κB, MAPK and TNFR1-induced apoptotic signaling. In breast cancer cells, TNF-α has been shown to activate NF-κB to promote tumor development through anti-apoptotic signaling (92). IL-6 is also a pro-inflammatory cytokine, binding to its receptor and activing the JAK1/STAT3 signaling pathway, resulting in transcription of anti-apoptotic genes (93). GM-CSF has been shown to both suppress and enhance tumor growth (94). GM-CSF production is stimulated by inflammatory cytokines, such as TNF-α and IL-6, and GM-CSF stimulation triggers downstream signaling leading to activation of STAT5 and MAPK pathways (95–97). IPA analysis showed varying levels of predicted activation of NF-κB complex in each experimental group, suggesting that other NF-κB family members are involved

in maintenance of dormancy and relapse as well. It is also important to consider that determining the exact effects of one NF-κB family member is difficult, due to their propensity to form many different combinations of homo-and heterodimers, with many displaying overlap in function (98). Taken together, the NF-κB p65 signaling pathway contributes to the survival signaling that allows MMC to avoid ADR-induced apoptosis, but other pathways likely crosstalk with this signaling which results in an optimal ratio of survival to apoptotic signaling that allows for dormancy to occur. Further investigation into these pathways, with gene analysis and additional gene knockouts, could provide insight into dormancy signaling in order to either prevent induction of dormancy, or maintain dormant cells in a dormant state for life, thus preventing recurrence.

NF-κB p65 also inhibits the immunomodulatory effects of ADR. Chemotherapeutic agents have been shown to cause changes in expression of proteins that alter the anti-tumor response (99). This is an additional benefit of chemotherapy that allows for better recognition of tumor cells by the immune system due to, for example, upregulation of tumor-specific antigens or antigen-presenting machinery such as MHC1 (100). Though NF-κB p65 did not have any effects on MHCI upregulation upon ADR treatment, our data supports findings in the field showing upregulation of MHCI in response to ADR treatment, which could be exploited for immunotherapy due to better tumor-antigen presentation on ADR-treated tumor cells (101). NF-κB p65 does, however, suppress expression of neu, with shNF-κB p65 showing increase in neu expression after ADR-treatment, compared to both the non-treated and treated SCR-MMC groups both *in vitro* and *in vivo*. Such findings suggest that NF-κB blockade could increase the efficacy of not only chemotherapeutic agents, but additional adjuvant hormone therapy and immunotherapy as well. Further experiments including the addition of the anti-HER2/neu drug,

trastuzumab, or immunotherapy following ADR treatment in shNF-κB p65 could confirm this hypothesis.

We have demonstrated that knockdown of tumor-intrinsic NF-κB signaling pathways can benefit the host by increasing ADR-sensitivity and prolonging relapse, but the same cannot be said for the extrinsic signaling effects of NF-κB knockdown in tumor cells. We demonstrated that tumors lacking NF-κB p65 show altered immune-cell infiltrate compared to SCR-MMC tumors. Though overall percentage of CD45+ immune cells showed no statistical differences between control and ADR-treated shNF-κB p65 tumors and SCR-MMC tumors, untreated shNF-κB p65 tumors showed a reduction in CD8+ T cells and increase in CD11b+ monocytes/macrophages. Increased CD8+ T cells has been shown to predict clinical outcome, with higher intratumoral CD8+ T lymphocytic infiltrate being associated with better clinical outcomes (102). In accordance with our data showing fewer CD8+ T cells, we also found a significant decrease in T cell expansion, *ex vivo,* and decrease in anti-tumor activity from shNF-κB p65-inoculated mice against MMC when cultured together. Our findings suggest that tumor-intrinsic NF-κB signaling pathways in tumor cells alone can decrease monocyte/macrophage infiltration and increase CD8+ lymphocytic infiltration, ultimately allowing for an effective CD8+ cytotoxic anti-tumor response.

Due to the aberrant activation of NF-κB found in tumor cells, there have been attempts to block NF-κB signaling through the development of NF-κB-inhibiting drugs. Tumor-intrinsic NF-κB signaling plays a dual function in cancer progression; while it provides a growth advantage to the tumor, it also promotes inflammation that increases immune signaling (41, 46). This dichotomy is likely, in part, the reason why attempts at blocking NF-κB tumor signaling through the development of NF-κB inhibitors have not been effective as a treatment, resulting in off-

target effects (88). Bortezomib, the first-in-class proteasome inhibitor, blocks the NF-κB pathway along with many other pathways that rely on ubiquitin degradation (88). Bortezomib is clinically approved for treatment against multiple myeloma and mantle-cell lymphoma, though whether or not this success is chiefly due to inhibition of NF-κB signaling or other pathways is unknown (103).

To our knowledge, this is the first study in which NF-κB gene knockdown or knockout was performed in tumor cells to study the effects of tumor-intrinsic inflammatory pathways on ADR-induced dormancy and recurrence. Drugs targeting the tumor-intrinsic NF-κB pathway, such as FDA-approved Bortezomib, could be used during neo-adjuvant chemotherapy and hormone therapy in order to prevent tumor cells from escaping the apoptotic effects of ADR and entering a dormant state that will eventually relapse. However, cation should be exercised when inhibiting tumor-intrinsic NF-κB p65 activity due to it's contribution to the anti-tumor immune response. Further studies are needed to corroborate the data presented here, which will hopefully answer some of these clinically relevant questions.

Future Directions

Our lab is continuing to investigate the role of tumor-intrinsic NF-κB signaling in dormancy and recurrence with our CRISPR-Cas9 NF-κB p65 knockout cell line. We plan to investigate the rate of relapse both *in vitro* and *in vivo* and hypothesize it will support our shRNA NF-κB p65 data. We also plan to do additional animal studies on immune-cell infiltrate in order to compare statistical differences between experimental and control groups. We will also be performing additional cytokine analysis on supernatant collected from different time points in the shRNA and CRISPR-Cas9 cell lines in order to determine the relationship of these cytokines to NF-κB p65 activity. Due to our discovery that NF-κB p65 inhibits some of the immunomodulatory effects of ADR, we will also investigate other molecules related to immune modulation such as HMGB-1, Rae-1, and CRT. Lastly, we will investigate the role of NF-κB p65 in ADR-induced drug-resistance by additionally treating cells with ADR during dormancy.

References

1. Howlader N, Noone AM, Krapcho M, Miller D, Bishop K, Altekruse SF, Kosary CL, Yu M, Ruhl J, Tatalovich Z, Mariotto A, Lewis DR, Chen HS, Feuer EJ, Cronin KA (eds). SEER Cancer Statistics Review, 1975-2013, National Cancer Institute. Bethesda, MD, http://seer.cancer.gov/csr/1975_2013/, based on November 2015 SEER data submission, posted to the SEER web site, April 2016.

2. Klein, C. A. Framework models of tumor dormancy from patient-derived observations - ClinicalKey. .

3. Klein, C. A. 2013. Selection and adaptation during metastatic cancer progression. *Nature* 501: 365–372.

4. 2005. Effects of chemotherapy and hormonal therapy for early breast cancer on recurrence and 15-year survival: an overview of the randomised trials. *The Lancet* 365: 1687–1717.

5. Callahan, R., and S. Hurvitz. 2011. HER2-Positive Breast Cancer: Current Management of Early, Advanced, and Recurrent Disease. *Curr. Opin. Obstet. Gynecol.* 23: 37–43.

6. Slamon, D. J., B. Leyland-Jones, S. Shak, H. Fuchs, V. Paton, A. Bajamonde, T. Fleming, W. Eiermann, J. Wolter, M. Pegram, J. Baselga, and L. Norton. 2001. Use of chemotherapy plus a monoclonal antibody against HER2 for metastatic breast cancer that overexpresses HER2. *N. Engl. J. Med.* 344: 783–792.

7. Arribas, J., J. Baselga, K. Pedersen, and J. L. Parra-Palau. 2011. p95HER2 and breast cancer. *Cancer Res.* 71: 1515–1519.

8. Meng, S., D. Tripathy, E. P. Frenkel, S. Shete, E. Z. Naftalis, J. F. Huth, P. D. Beitsch, M. Leitch, S. Hoover, D. Euhus, B. Haley, L. Morrison, T. P. Fleming, D. Herlyn, L. W. M. M.

Terstappen, T. Fehm, T. F. Tucker, N. Lane, J. Wang, and J. W. Uhr. 2004. Circulating tumor cells in patients with breast cancer dormancy. *Clin. Cancer Res. Off. J. Am. Assoc. Cancer Res.* 10: 8152–8162.

9. Pound, C. R., A. W. Partin, M. A. Eisenberger, D. W. Chan, J. D. Pearson, and P. C. Walsh. 1999. Natural history of progression after PSA elevation following radical prostatectomy. *JAMA* 281: 1591–1597.

10. Faries, M. B., S. Steen, X. Ye, M. Sim, and D. L. Morton. 2013. Late recurrence in melanoma: clinical implications of lost dormancy. *J. Am. Coll. Surg.* 217: 27-34-36.

11. Press, O. W., J. P. Leonard, B. Coiffier, R. Levy, and J. Timmerman. 2001. Immunotherapy of Non-Hodgkin's Lymphomas. *ASH Educ. Program Book* 2001: 221–240.

12. Müller, V., N. Stahmann, S. Riethdorf, T. Rau, T. Zabel, A. Goetz, F. Jänicke, and K. Pantel. 2005. Circulating tumor cells in breast cancer: correlation to bone marrow micrometastases, heterogeneous response to systemic therapy and low proliferative activity. *Clin. Cancer Res. Off. J. Am. Assoc. Cancer Res.* 11: 3678–3685.

13. Gebauer, G., T. Fehm, E. Merkle, E. P. Beck, N. Lang, and W. Jäger. 2001. Epithelial cells in bone marrow of breast cancer patients at time of primary surgery: clinical outcome during long-term follow-up. *J. Clin. Oncol. Off. J. Am. Soc. Clin. Oncol.* 19: 3669–3674.

14. van der Toom, E. E., J. E. Verdone, and K. J. Pienta. 2016. Disseminated tumor cells and dormancy in prostate cancer metastasis. *Curr. Opin. Biotechnol.* 40: 9–15.

15. Aguirre-Ghiso, J. A. 2007. Models, mechanisms and clinical evidence for cancer dormancy. *Nat. Rev. Cancer* 7: 834–846.

16. Weinhold, K. J., L. T. Goldstein, and E. F. Wheelock. 1979. The tumor dormant state. Quantitation of L5178Y cells and host immune responses during the establishment and course of dormancy in syngeneic DBA/2 mice. *J. Exp. Med.* 149: 732–744.

17. Payne, K. K., R. C. Keim, L. Graham, M. O. Idowu, W. Wan, X.-Y. Wang, A. A. Toor, H. D. Bear, and M. H. Manjili. 2016. Tumor-reactive immune cells protect against metastatic tumor and induce immunoediting of indolent but not quiescent tumor cells. *J. Leukoc. Biol.* 100: 625–635.

18. Dunn, G. P., A. T. Bruce, H. Ikeda, L. J. Old, and R. D. Schreiber. 2002. Cancer immunoediting: from immunosurveillance to tumor escape. *Nat. Immunol.* 3: 991–998.

19. Dunn, G. P., L. J. Old, and R. D. Schreiber. 2004. The three Es of cancer immunoediting. *Annu. Rev. Immunol.* 22: 329–360.

20. Gelao, L., C. Criscitiello, L. Fumagalli, M. Locatelli, S. Manunta, A. Esposito, I. Minchella, A. Goldhirsch, and G. Curigliano. 2013. Tumour dormancy and clinical implications in breast cancer. *ecancermedicalscience* 7.

21. Mellor, H. R., D. J. P. Ferguson, and R. Callaghan. 2005. A model of quiescent tumour microregions for evaluating multicellular resistance to chemotherapeutic drugs. *Br. J. Cancer* 93: 302–309.

22. Thorn, C. F., C. Oshiro, S. Marsh, T. Hernandez-Boussard, H. McLeod, T. E. Klein, and R. B. Altman. 2011. Doxorubicin pathways: pharmacodynamics and adverse effects. *Pharmacogenet. Genomics* 21: 440–446.

23. KAWANO, M., K. TANAKA, I. ITONAGA, T. IWASAKI, M. MIYAZAKI, S. IKEDA, and H. TSUMURA. 2016. Dendritic cells combined with doxorubicin induces immunogenic cell death and exhibits antitumor effects for osteosarcoma. *Oncol. Lett.* 11: 2169–2175.

24. Sistigu, A., T. Yamazaki, E. Vacchelli, K. Chaba, D. P. Enot, J. Adam, I. Vitale, A. Goubar, E. E. Baracco, C. Remédios, L. Fend, D. Hannani, L. Aymeric, Y. Ma, M. Niso-Santano, O. Kepp, J. L. Schultze, T. Tüting, F. Belardelli, L. Bracci, V. La Sorsa, G. Ziccheddu, P. Sestili, F. Urbani, M. Delorenzi, M. Lacroix-Triki, V. Quidville, R. Conforti, J.-P. Spano, L. Pusztai, V. Poirier-Colame, S. Delaloge, F. Penault-Llorca, S. Ladoire, L. Arnould, J. Cyrta, M.-C. Dessoliers, A. Eggermont, M. E. Bianchi, M. Pittet, C. Engblom, C. Pfirschke, X. Préville, G. Uzè, R. D. Schreiber, M. T. Chow, M. J. Smyth, E. Proietti, F. André, G. Kroemer, and L. Zitvogel. 2014. Cancer cell-autonomous contribution of type I interferon signaling to the efficacy of chemotherapy. *Nat. Med.* 20: 1301–1309.

25. Dufour, J. H., M. Dziejman, M. T. Liu, J. H. Leung, T. E. Lane, and A. D. Luster. 2002. IFN-gamma-inducible protein 10 (IP-10; CXCL10)-deficient mice reveal a role for IP-10 in effector T cell generation and trafficking. *J. Immunol. Baltim. Md 1950* 168: 3195–3204.

26. Wang, S., and S.-Y. Lin. 2013. Tumor dormancy: potential therapeutic target in tumor recurrence and metastasis prevention. *Exp. Hematol. Oncol.* 2: 29.

27. Hickson, J. A., D. Huo, D. J. Vander Griend, A. Lin, C. W. Rinker-Schaeffer, and S. D. Yamada. 2006. The p38 kinases MKK4 and MKK6 suppress metastatic colonization in human ovarian carcinoma. *Cancer Res.* 66: 2264–2270.

28. Aguirre-Ghiso, J. A., L. Ossowski, and S. K. Rosenbaum. 2004. Green fluorescent protein tagging of extracellular signal-regulated kinase and p38 pathways reveals novel dynamics of pathway activation during primary and metastatic growth. *Cancer Res.* 64: 7336–7345.

29. Xia, Z., M. Dickens, J. Raingeaud, R. J. Davis, and M. E. Greenberg. 1995. Opposing effects of ERK and JNK-p38 MAP kinases on apoptosis. *Science* 270: 1326–1331.

30. Ranganathan, A. C., L. Zhang, A. P. Adam, and J. A. Aguirre-Ghiso. 2006. Functional coupling of p38-induced up-regulation of BiP and activation of RNA-dependent protein kinase-like endoplasmic reticulum kinase to drug resistance of dormant carcinoma cells. *Cancer Res.* 66: 1702–1711.

31. Patel, S. A., S. H. Ramkissoon, M. Bryan, L. F. Pliner, G. Dontu, P. S. Patel, S. Amiri, S. R. Pine, and P. Rameshwar. 2012. Delineation of breast cancer cell hierarchy identifies the subset responsible for dormancy. *Sci. Rep.* 2: 906.

32. Ghajar, C. M. 2015. Metastasis prevention by targeting the dormant niche. *Nat. Rev. Cancer* 15: 238–247.

33. Kobayashi, A., H. Okuda, F. Xing, P. R. Pandey, M. Watabe, S. Hirota, S. K. Pai, W. Liu, K. Fukuda, C. Chambers, A. Wilber, and K. Watabe. 2011. Bone morphogenetic protein 7 in dormancy and metastasis of prostate cancer stem-like cells in bone. *J. Exp. Med.* 208: 2641–2655.

34. Bragado, P., Y. Estrada, F. Parikh, S. Krause, C. Capobianco, H. G. Farina, D. M. Schewe, and J. A. Aguirre-Ghiso. 2013. TGFβ2 dictates disseminated tumour cell fate in target organs through TGFβ-RIII and p38α/β signalling. *Nat. Cell Biol.* 15: 1351–1361.

35. Lu, X., E. Mu, Y. Wei, S. Riethdorf, Q. Yang, M. Yuan, J. Yan, Y. Hua, B. J. Tiede, X. Lu, B. G. Haffty, K. Pantel, J. Massagué, and Y. Kang. 2011. VCAM-1 promotes osteolytic expansion of indolent bone micrometastasis of breast cancer by engaging α4β1-positive osteoclast progenitors. *Cancer Cell* 20: 701–714.

36. Dollé, L., I. El Yazidi-Belkoura, E. Adriaenssens, V. Nurcombe, and H. Hondermarck. 2003. Nerve growth factor overexpression and autocrine loop in breast cancer cells. *Oncogene* 22: 5592–5601.

37. Sampattavanich, S. 2011. A general method for studying autocrine signaling and its impact on cancer cell growth. .

38. Lin, L., and E. H. Baehrecke. 2015. Autophagy, cell death, and cancer. *Mol. Cell. Oncol.* 2.

39. Amaravadi, R. K., and C. B. Thompson. 2007. The roles of therapy-induced autophagy and necrosis in cancer treatment. *Clin. Cancer Res. Off. J. Am. Assoc. Cancer Res.* 13: 7271–7279.

40. Amaravadi, R. K., D. Yu, J. J. Lum, T. Bui, M. A. Christophorou, G. I. Evan, A. Thomas-Tikhonenko, and C. B. Thompson. 2007. Autophagy inhibition enhances therapy-induced apoptosis in a Myc-induced model of lymphoma. *J. Clin. Invest.* 117: 326–336.

41. Mantovani, A., P. Allavena, A. Sica, and F. Balkwill. 2008. Cancer-related inflammation. *Nature* 454: 436–444.

42. Landskron, G., M. De la Fuente, P. Thuwajit, C. Thuwajit, and M. A. Hermoso. 2014. Chronic Inflammation and Cytokines in the Tumor Microenvironment. *J. Immunol. Res.* 2014: e149185.

43. Popa, C., M. G. Netea, P. L. C. M. van Riel, J. W. M. van der Meer, and A. F. H. Stalenhoef. 2007. The role of TNF-alpha in chronic inflammatory conditions, intermediary metabolism, and cardiovascular risk. *J. Lipid Res.* 48: 751–762.

44. Heikkilä, K., S. Ebrahim, and D. A. Lawlor. 2008. Systematic review of the association between circulating interleukin-6 (IL-6) and cancer. *Eur. J. Cancer Oxf. Engl. 1990* 44: 937–945.

45. Baron, J. A., and R. S. Sandler. 2000. Nonsteroidal anti-inflammatory drugs and cancer prevention. *Annu. Rev. Med.* 51: 511–523.

46. Balkwill, F., and A. Mantovani. 2001. Inflammation and cancer: back to Virchow? *Lancet Lond. Engl.* 357: 539–545.

47. Rossi, D., and A. Zlotnik. 2000. The biology of chemokines and their receptors. *Annu. Rev. Immunol.* 18: 217–242.

48. Tyler, D. S., G. M. Francis, M. Frederick, A. H. Tran, N. G. Ordóñez, J. L. Smith, O. Eton, M. Ross, and E. A. Grimm. 1995. Interleukin-1 production in tumor cells of human melanoma surgical specimens. *J. Interferon Cytokine Res. Off. J. Int. Soc. Interferon Cytokine Res.* 15: 331–340.

49. Leek, R. D., R. Landers, S. B. Fox, F. Ng, A. L. Harris, and C. E. Lewis. 1998. Association of tumour necrosis factor alpha and its receptors with thymidine phosphorylase expression in invasive breast carcinoma. *Br. J. Cancer* 77: 2246–2251.

50. Sasser, A. K., N. J. Sullivan, A. W. Studebaker, L. F. Hendey, A. E. Axel, and B. M. Hall. 2007. Interleukin-6 is a potent growth factor for ER-alpha-positive human breast cancer. *FASEB J. Off. Publ. Fed. Am. Soc. Exp. Biol.* 21: 3763–3770.

51. Breast Cancer Immunology : Oncology Times. *LWW* .

52. Rabinovich, G. A., D. Gabrilovich, and E. M. Sotomayor. 2007. IMMUNOSUPPRESSIVE STRATEGIES THAT ARE MEDIATED BY TUMOR CELLS. *Annu. Rev. Immunol.* 25: 267–296.

53. Targeting Cancer-Related Inflammation in the Era of Immunotherapy. *PubMed J.* .

54. Hagemann, T., T. Lawrence, I. McNeish, K. A. Charles, H. Kulbe, R. G. Thompson, S. C. Robinson, and F. R. Balkwill. 2008. “Re-educating” tumor-associated macrophages by targeting NF-κB. *J. Exp. Med.* 205: 1261–1268.

55. Richmond, A., and H. G. Thomas. 1986. Purification of melanoma growth stimulatory activity. *J. Cell. Physiol.* 129: 375–384.

56. Sparmann, A., and D. Bar-Sagi. 2004. Ras-induced interleukin-8 expression plays a critical role in tumor growth and angiogenesis. *Cancer Cell* 6: 447–458.

57. Liu, J., G. Yang, J. A. Thompson-Lanza, A. Glassman, K. Hayes, A. Patterson, R. T. Marquez, N. Auersperg, Y. Yu, W. C. Hahn, G. B. Mills, and R. C. Bast. 2004. A genetically defined model for human ovarian cancer. *Cancer Res.* 64: 1655–1663.

58. Balamurugan, K. 2016. HIF-1 at the crossroads of hypoxia, inflammation, and cancer. *Int. J. Cancer* 138: 1058–1066.

59. Caamaño, J., and C. A. Hunter. 2002. NF-κB Family of Transcription Factors: Central Regulators of Innate and Adaptive Immune Functions. *Clin. Microbiol. Rev.* 15: 414–429.

60. NF-κB Signaling Pathway | Cell Signaling Technology. .

61. Schmid, J. A., and A. Birbach. 2008. IkappaB kinase beta (IKKbeta/IKK2/IKBKB)--a key molecule in signaling to the transcription factor NF-kappaB. *Cytokine Growth Factor Rev.* 19: 157–165.

62. Sun, S.-C. 2011. Non-canonical NF-κB signaling pathway. *Cell Res.* 21: 71–85.

63. La Rosa, F. A., J. W. Pierce, and G. E. Sonenshein. 1994. Differential regulation of the c-myc oncogene promoter by the NF-kappa B rel family of transcription factors. *Mol. Cell. Biol.* 14: 1039–1044.

64. Perkins, N. D. 1997. Achieving transcriptional specificity with NF-kappa B. *Int. J. Biochem. Cell Biol.* 29: 1433–1448.

65. Disis, M. L. 2010. Immune Regulation of Cancer. *J. Clin. Oncol.* 28: 4531–4538.

66. Huber, M. A., N. Azoitei, B. Baumann, S. Grünert, A. Sommer, H. Pehamberger, N. Kraut, H. Beug, and T. Wirth. 2004. NF-κB is essential for epithelial-mesenchymal transition and metastasis in a model of breast cancer progression. *J. Clin. Invest.* 114: 569–581.

67. Xie, T.-X., Z. Xia, N. Zhang, W. Gong, and S. Huang. 2010. Constitutive NF-kappaB activity regulates the expression of VEGF and IL-8 and tumor angiogenesis of human glioblastoma. *Oncol. Rep.* 23: 725–732.

68. Ben-Neriah, Y., and M. Karin. 2011. Inflammation meets cancer, with NF-κB as the matchmaker. *Nat. Immunol.* 12: 715–723.

69. Oeckinghaus, A., and S. Ghosh. 2009. The NF-κB Family of Transcription Factors and Its Regulation. *Cold Spring Harb. Perspect. Biol.* 1.

70. Neurath, M. F., I. Fuss, G. Schürmann, S. Pettersson, K. Arnold, H. Müller-Lobeck, W. Strober, C. Herfarth, and K. H. Büschenfelde. 1998. Cytokine gene transcription by NF-kappa B family members in patients with inflammatory bowel disease. *Ann. N. Y. Acad. Sci.* 859: 149–159.

71. Courtois, G., and T. D. Gilmore. 2006. Mutations in the NF-kappaB signaling pathway: implications for human disease. *Oncogene* 25: 6831–6843.

72. Grivennikov, S. I., and M. Karin. 2010. Dangerous liaisons: STAT3 and NF-kappaB collaboration and crosstalk in cancer. *Cytokine Growth Factor Rev.* 21: 11–19.

73. Levy, D. E., and C. Lee. 2002. What does Stat3 do? *J. Clin. Invest.* 109: 1143–1148.

74. Webster, G. A., and N. D. Perkins. 1999. Transcriptional cross talk between NF-kappaB and p53. *Mol. Cell. Biol.* 19: 3485–3495.

75. Guy, C. T., M. A. Webster, M. Schaller, T. J. Parsons, R. D. Cardiff, and W. J. Muller. 1992. Expression of the neu protooncogene in the mammary epithelium of transgenic mice induces metastatic disease. *Proc. Natl. Acad. Sci. U. S. A.* 89: 10578–10582.

76. Kmieciak, M., K. L. Knutson, C. I. Dumur, and M. H. Manjili. 2007. HER-2/neu antigen loss and relapse of mammary carcinoma are actively induced by T cell-mediated anti-tumor immune responses. *Eur. J. Immunol.* 37: 675–685.

77. Ascierto, M. L., M. Kmieciak, M. O. Idowu, R. Manjili, Y. Zhao, M. Grimes, C. Dumur, E. Wang, V. Ramakrishnan, X.-Y. Wang, H. D. Bear, F. M. Marincola, and M. H. Manjili. 2012. A signature of immune function genes associated with recurrence-free survival in breast cancer patients. *Breast Cancer Res. Treat.* 131: 871–880.

78. Kmieciak, M., D. Basu, K. K. Payne, A. Toor, A. Yacoub, X.-Y. Wang, L. Smith, H. D. Bear, and M. H. Manjili. 2011. Activated NKT cells and NK cells render T cells resistant to myeloid-derived suppressor cells and result in an effective adoptive cellular therapy against breast cancer in the FVBN202 transgenic mouse. *J. Immunol. Baltim. Md 1950* 187: 708–717.

79. Jia, L., G. Gopinathan, J. T. Sukumar, and J. G. Gribben. 2012. Blocking Autophagy Prevents Bortezomib-Induced NF-κB Activation by Reducing I-κBα Degradation in Lymphoma Cells. *PLoS ONE* 7.

80. Pachynski, R. K., A. Scholz, J. Monnier, E. C. Butcher, and B. A. Zabel. 2015. Evaluation of Tumor-infiltrating Leukocyte Subsets in a Subcutaneous Tumor Model. *J. Vis. Exp. JoVE* .

81. Liang, X., J. Tang, Y. Liang, R. Jin, and X. Cai. 2014. Suppression of autophagy by chloroquine sensitizes 5-fluorouracil-mediated cell death in gallbladder carcinoma cells. *Cell Biosci.* 4: 10.

82. Maes, H., A. Kuchnio, P. Carmeliet, and P. Agostinis. 2014. How to teach an old dog new tricks: Autophagy-independent action of chloroquine on the tumor vasculature. *Autophagy* 10: 2082–2084.

83. Souba, W. W. 1993. Glutamine and cancer. *Ann. Surg.* 218: 715–728.

84. DeBerardinis, R. J., and T. Cheng. 2010. Q's next: the diverse functions of glutamine in metabolism, cell biology and cancer. *Oncogene* 29: 313–324.

85. Huang, W., W. Choi, Y. Chen, Q. Zhang, H. Deng, W. He, and Y. Shi. 2013. A proposed role for glutamine in cancer cell growth through acid resistance. *Cell Res.* 23: 724–727.

86. Jiang, X.-J., K.-K. Huang, M. Yang, L. Qiao, Q. Wang, J.-Y. Ye, H.-S. Zhou, Z.-S. Yi, F.-Q. Wu, Z.-X. Wang, Q.-X. Zhao, and F.-Y. Meng. 2012. Synergistic effect of panobinostat and bortezomib on chemoresistant acute myelogenous leukemia cells via AKT and NF-κB pathways. *Cancer Lett.* 326: 135–142.

87. Katsman, A., K. Umezawa, and B. Bonavida. 2009. Chemosensitization and immunosensitization of resistant cancer cells to apoptosis and inhibition of metastasis by the specific NF-kappaB inhibitor DHMEQ. *Curr. Pharm. Des.* 15: 792–808.

88. DiDonato, J. A., F. Mercurio, and M. Karin. 2012. NF-κB and the link between inflammation and cancer. *Immunol. Rev.* 246: 379–400.

89. Jiao, X., L. Wood, M. Lindman, S. Jones, P. Buckhaults, K. Polyak, S. Sukumar, H. Carter, D. Kim, R. Karchin, and T. Sjöblom. 2012. Somatic Mutations in the Notch, NF-KB, PIK3CA, and Hedgehog Pathways in Human Breast Cancers. *Genes. Chromosomes Cancer* 51: 480–489.

90. Anisowicz, A., L. Bardwell, and R. Sager. 1987. Constitutive overexpression of a growth-regulated gene in transformed Chinese hamster and human cells. *Proc. Natl. Acad. Sci.* 84: 7188–7192.

91. Richmond, A., and H. G. Thomas. 1988. Melanoma growth stimulatory activity: Isolation from human melanoma tumors and characterization of tissue distribution. *J. Cell. Biochem.* 36: 185–198.

92. Zhou, B. P., M. C. Hu, S. A. Miller, Z. Yu, W. Xia, S. Y. Lin, and M. C. Hung. 2000. HER-2/neu blocks tumor necrosis factor-induced apoptosis via the Akt/NF-kappaB pathway. *J. Biol. Chem.* 275: 8027–8031.

93. Murray, P. J. 2007. The JAK-STAT signaling pathway: input and output integration. *J. Immunol. Baltim. Md 1950* 178: 2623–2629.

94. Hong, I.-S. 2016. Stimulatory versus suppressive effects of GM-CSF on tumor progression in multiple cancer types. *Exp. Mol. Med.* 48: e242.

95. Suh, H.-S., M.-O. Kim, and S. C. Lee. 2005. Inhibition of granulocyte-macrophage colony-stimulating factor signaling and microglial proliferation by anti-CD45RO: role of Hck tyrosine kinase and phosphatidylinositol 3-kinase/Akt. *J. Immunol. Baltim. Md 1950* 174: 2712–2719.

96. Sonderegger, I., G. Iezzi, R. Maier, N. Schmitz, M. Kurrer, and M. Kopf. 2008. GM-CSF mediates autoimmunity by enhancing IL-6-dependent Th17 cell development and survival. *J. Exp. Med.* 205: 2281–2294.

97. Atanga, E., S. Dolder, T. Dauwalder, A. Wetterwald, and W. Hofstetter. 2011. TNFα inhibits the development of osteoclasts through osteoblast-derived GM-CSF. *Bone* 49: 1090–1100.

98. Hayden, M. S., and S. Ghosh. 2008. Shared Principles in NF-κB Signaling. *Cell* 132: 344–362.

99. Nars, M. S., and R. Kaneno. 2013. Immunomodulatory effects of low dose chemotherapy and perspectives of its combination with immunotherapy. *Int. J. Cancer* 132: 2471–2478.

100. Restifo, N. P., Y. Kawakami, F. Marincola, P. Shamamian, A. Taggarse, F. Esquivel, and S. A. Rosenberg. 1993. Molecular Mechanisms Used by Tumors to Escape Immune Recognition: Immunogenetherapy and the Cell Biology of Major Histocompatibility Complex Class I. *J. Immunother. Emphas. Tumor Immunol. Off. J. Soc. Biol. Ther.* 14: 182–190.

101. Mantia-Smaldone, G., L. Ronner, A. Blair, V. Gamerman, C. Morse, S. Orsulic, S. Rubin, P. Gimotty, and S. Adams. 2014. The immunomodulatory effects of pegylated liposomal doxorubicin are amplified in BRCA1− deficient ovarian tumors and can be exploited to improve treatment response in a mouse model. *Gynecol. Oncol.* 133: 584–590.

102. Mahmoud, S. M. A., E. C. Paish, D. G. Powe, R. D. Macmillan, M. J. Grainge, A. H. S. Lee, I. O. Ellis, and A. R. Green. 2011. Tumor-Infiltrating CD8+ Lymphocytes Predict Clinical Outcome in Breast Cancer. *J. Clin. Oncol.* 29: 1949–1955.

103. D. Chen, M. F. Bortezomib as the First Proteasome Inhibitor Anticancer Drug: Current Status and Future Perspectives. *http://www.eurekaselect.com.proxy.library.vcu.edu* .

Vita

Savannah Elizabeth Butler was born on November 23, 1991 in San Diego, California. After finishing high school in 2010, she received her Bachelor of Science in Biology from the College of William and Mary, Williamsburg, Virginia in 2014.